


## Quantum geometry induced anapole superconductivity

Taisei Kitamura <sup>\*</sup>, Shota Kanasugi , Michiya Chazono , and Youichi Yanase  
*Department of Physics, Graduate School of Science, Kyoto University, Kyoto 606-8502, Japan*

 (Received 4 October 2022; revised 3 May 2023; accepted 5 May 2023; published 14 June 2023)

Anapole superconductivity recently proposed for multiband superconductors [S. Kanasugi and Y. Yanase, *Commun. Phys.* **5**, 39 (2022)] is a key feature of time-reversal ( $\mathcal{T}$ ) symmetry broken polar superconductors. The anapole moment was shown to arise from the asymmetric Bogoliubov spectrum, which induces finite center of mass momenta of Cooper pairs at the zero magnetic field. In this paper, we show an alternative mechanism of anapole superconductivity: the quantum geometry induces the anapole moment when the interband pairing and Berry connection are finite. Thus, the anapole superconductivity is a ubiquitous feature of  $\mathcal{T}$ -broken multiband polar superconductors. Applying the theory to a minimal model of  $\text{UTe}_2$ , we demonstrate the quantum geometry induced anapole superconductivity. Furthermore, we show the Bogoliubov Fermi surfaces (BFS) in an anapole superconducting state and predict an unusual temperature dependence of BFS due to the quantum geometry. Experimental verification of these phenomena may clarify the superconducting state in  $\text{UTe}_2$  and reveal the ubiquitous importance of quantum geometry in exotic superconductors.

DOI: [10.1103/PhysRevB.107.214513](https://doi.org/10.1103/PhysRevB.107.214513)

### I. INTRODUCTION

Parity-mixed superconductors, in which even- and odd-parity pairings coexist, are attracting much attention, as the parity-mixing phenomena are closely related to the space inversion ( $\mathcal{P}$ ) symmetry breaking. Stimulated by the discovery of noncentrosymmetric superconductivity in heavy fermions and artificial heterostructures, time-reversal ( $\mathcal{T}$ ) symmetric parity-mixed pairing states such as the  $s + p$ -wave state have been investigated intensively [1,2]. For a long time, studies focused on the crystals lacking the  $\mathcal{P}$  symmetry allowing an antisymmetric spin-orbit coupling (ASOC). Consequently, the Rashba superconductor and the Ising superconductor have become fundamental concepts in condensed matter physics [1,2].

On the other hand, centrosymmetric crystals were recently shown to be an intriguing platform of spontaneously  $\mathcal{P}$ -symmetry breaking superconductivity [3–5]. In the absence of the ASOC, additional  $\mathcal{T}$ -symmetry breaking is expected [3–5] as the  $\pm\pi/2$  phase difference between even- and odd-parity pairing potentials, such as the  $s + ip$ -wave pairing state, is energetically favored. As a result, both the  $\mathcal{P}$  and  $\mathcal{T}$  symmetry are broken while the combined  $\mathcal{PT}$  symmetry is preserved. The three-dimensional  $s + ip$ -wave pairing state in single-band superconductors was theoretically studied as a superconducting analog [6–8] of axion insulators [9,10]. Such a pairing state in  $\text{Sr}_2\text{RuO}_4$  was theoretically proposed [11]. Furthermore, a recently discovered candidate for spin-triplet superconductor  $\text{UTe}_2$  [12,13] is predicted to realize the  $s + ip$ -wave pairing state [14], as it is consistent with the experimentally observed multiple superconducting phases [15–21] and multiple magnetic fluctuations [22–27].

Clarification of the  $\mathcal{PT}$ -symmetric parity-mixed superconductivity has been awaited to uncover an exotic state of matter. However, properties of the  $\mathcal{PT}$ -symmetric parity-mixed superconductivity are almost unresolved. In particular, theoretical studies of *multiband* superconductors have not been carried out except for Ref. [28], although it is known that intriguing superconducting phenomena such as the intrinsic polar Kerr effect [29–31] and Bogoliubov Fermi surfaces (BFS) [32,33] may appear from multiband properties. In Ref. [28], the anapole superconductivity was discussed as an exotic feature of the  $\mathcal{PT}$ -symmetric parity-mixed pairing state in multiband superconductors. If some conditions are satisfied, an asymmetric Bogoliubov spectrum (BS) arises from the interband pairing [28]. When the symmetry of superconductivity has a polar property, such as in the  $A_g + iB_{3u}$  pairing state proposed for  $\text{UTe}_2$  [14], the asymmetric BS induces an effective anapole moment, which is defined as the first-order coefficient of the free energy in terms of the center of mass momenta of Cooper pairs. The anapole moment characterizes the anapole superconductivity as it does the anapole order in magnetic materials [34–38] and the nucleus [39].

The anapole moment is a polar and  $\mathcal{T}$ -odd vector [34], which shares the symmetry as the velocity and momentum. Therefore, it is not surprising that the effective anapole moment induces finite center of mass momenta of Cooper pairs  $\mathbf{q}$  even in the absence of the magnetic field. The mechanism of finite- $\mathbf{q}$  pairing is different from the Fulde-Ferrell-Larkin-Ovchinnikov (FFLO) superconductivity [40,41] and helical superconductivity [1,2], which require a finite magnetic field. For example, helical superconductivity can be stabilized in parity-mixed  $s + p$ -wave pairing states of noncentrosymmetric superconductors [1,2,42]. However,  $s + p$ -wave pairing does not cause  $\mathcal{T}$ -symmetry breaking which is needed for helical superconductivity, and therefore, an external magnetic field has to be applied. In contrast,  $s + ip$ -wave pairing

\*kitamura.taisei.67m@st.kyoto-u.ac.jp

intrinsically breaks  $\mathcal{P}$ - and  $\mathcal{T}$ -symmetry and may stabilize finite- $\mathbf{q}$  pairing anapole superconductivity in the field-free condition.

Therefore, in contrast to the FFLO and helical superconductivity, the anapole superconductivity can be studied with avoiding experimental difficulties due to vortices induced by an external magnetic field. For instance, the anapole domain switching [28], superconducting piezoelectric effect [43,44], and Josephson effect [45,46] may uncover intrinsic properties of anapole superconductivity. Therefore, the anapole superconductivity may be the key to elucidating the  $\mathcal{PT}$ -symmetric parity-mixed pairing state, and it may realize and clarify the finite- $\mathbf{q}$  pairing state which has been searched for a long time [1,2,47].

In this paper, we show that the anapole superconductivity is a ubiquitous feature more than revealed in the previous paper [28], considering the *quantum geometry* extensively studied in various fields [37,38,48–59]. Recently, an essential role of the quantum geometry in the superfluid weight, namely, the second-order derivative of the free energy, has been revealed [60–63]. Thus, it is naturally expected that the quantum geometry may be essential for the anapole superconductivity.

First, we provide a thorough formulation of the anapole moment based on the Bardeen-Cooper-Schrieffer (BCS) mean-field theory. The obtained formula contains two terms; one is the geometric term and the other is the group velocity term. Only a part of the group velocity term was derived in the previous literature [28]. Based on the general two-band model with the Kramers degeneracy, the microscopic origin of the geometric term is revealed to be the interband pairing and the Berry connection, while the group velocity term is induced by the asymmetric BS. Then, applying the theory to a model of  $\text{UTE}_2$ , we demonstrate the quantum geometry induced anapole superconductivity. Moreover, we show unique features of anapole superconductivity. When the system has a small gap minimum as expected for  $\text{UTE}_2$  [13], the anapole moment induces the BFS. The BFS may show a reappearing behavior as decreasing the temperature, causing anomalies in the density of states (DOS) and thermodynamic quantities.

## II. GENERAL FORMULA FOR ANAPOLE MOMENT

An order parameter of the anapole superconductivity is the anapole moment which is defined by the first-order coefficient of the free energy with respect to  $\mathbf{q}$ . In the previous study [28], the anapole moment is derived only when the  $\mathbf{k}$ -derivative of the normal-state Hamiltonian is proportional to the identity matrix, namely,  $\partial_\mu H_{\mathbf{k}} \propto \mathbf{1}$ . We adopt the notation  $\partial_\mu = \partial_{k_\mu}$ , and  $H_{\mathbf{k}}$  is the matrix representation of the single-particle Hamiltonian. Below, we formulate the anapole moment in the general case based on the BCS mean-field theory.

The normal state is assumed to be  $\mathcal{P}$  and  $\mathcal{T}$  symmetric, and therefore,  $H_{\mathbf{k}} = U_{\mathcal{T}} H_{-\mathbf{k}}^T U_{\mathcal{T}}^\dagger$  is satisfied, where  $U_{\mathcal{T}} = i\sigma_y \otimes \mathbf{1}$  is the unitary part of the  $\mathcal{T}$  operator with the Pauli matrix for the spin space  $\sigma_\mu$  ( $\mu = 0, x, y, z$ ). Thus, the Bogoliubov–de Gennes (BdG) Hamiltonian for a finite- $\mathbf{q}$  pairing state can be written as (see Appendix A)

$$\hat{H}^{\text{BdG}} = \frac{1}{2} \sum_{\mathbf{k}} \hat{\Psi}_{\mathbf{k},\mathbf{q}}^\dagger H_{\mathbf{k},\mathbf{q}}^{\text{BdG}} \hat{\Psi}_{\mathbf{k},\mathbf{q}}, \quad (1)$$

$$H_{\mathbf{k},\mathbf{q}}^{\text{BdG}} = \begin{pmatrix} H_{\mathbf{k}+\mathbf{q}} & \Delta_{\mathbf{k}} \\ \Delta_{\mathbf{k}}^\dagger & -H_{\mathbf{k}-\mathbf{q}} \end{pmatrix}, \quad (2)$$

$$\hat{\Psi}_{\mathbf{k},\mathbf{q}}^\dagger = (\hat{c}_{\mathbf{k}+\mathbf{q}}^\dagger \quad \hat{c}_{-\mathbf{k}+\mathbf{q}}^T U_{\mathcal{T}}^\dagger). \quad (3)$$

Here, we denote  $\hat{c}_{\mathbf{k}}^\dagger = (\hat{c}_{\uparrow 1\mathbf{k}}^\dagger \cdots \hat{c}_{\uparrow f\mathbf{k}}^\dagger \quad \hat{c}_{\downarrow 1\mathbf{k}}^\dagger \cdots \hat{c}_{\downarrow f\mathbf{k}}^\dagger)$ , where  $\hat{c}_{\sigma l\mathbf{k}}^\dagger$  is the creation operator for spin  $\sigma$  and the other internal degree of freedom  $l$ . We consider general cases, including multi-orbital and multi-sublattice systems, and  $f$  is the total number of degrees of freedom other than spin.

The off-diagonal part  $\Delta_{\mathbf{k}} = \Delta_{\mathbf{k}}^g + \Delta_{\mathbf{k}}^u$  is the gap function in the matrix representation, where  $\Delta_{\mathbf{k}}^{g(u)}$  is the  $\mathcal{P}$ -even (-odd) component of the pair potential. Coexistence of Cooper pairs with different parities, i.e., parity-mixed state, leads to broken  $\mathcal{P}$  symmetry. Furthermore, the  $\mathcal{T}$ -symmetry breaking is theoretically predicted [3–5], when the normal state preserves the  $\mathcal{P}$  symmetry. Thus, we assume the  $\pm\pi/2$  phase difference between  $\Delta_{\mathbf{k}}^g$  and  $\Delta_{\mathbf{k}}^u$ , consistent with the theoretical prediction [3–5]. As a result the  $\mathcal{P}$  and  $\mathcal{T}$  symmetry are broken by the parity-mixed gap function while the  $\mathcal{PT}$  symmetry is preserved. In addition, to make the anapole moment finite, throughout the paper, we assume the gap function  $\Delta_{\mathbf{k}}$  belongs to polar irreducible representation.

Expanding the free energy by  $\mathbf{q}$  as  $F_{\mathbf{q}} = T \cdot \mathbf{q} + \cdots$ , we obtain the anapole moment as

$$T_\mu = \frac{1}{2} \sum_{\mathbf{k}} \sum_a f(E_{a\mathbf{k}}) \langle \psi_{a\mathbf{k}} | \partial_\mu H_{\mathbf{k}}^+ | \psi_{a\mathbf{k}} \rangle, \quad (4)$$

$$H_{\mathbf{k}}^+ = \begin{pmatrix} H_{\mathbf{k}} & 0 \\ 0 & H_{\mathbf{k}} \end{pmatrix}. \quad (5)$$

Here, we use the eigenvalue equation  $H_{\mathbf{k}}^{\text{BdG}} | \psi_{a\mathbf{k}} \rangle = E_{a\mathbf{k}} | \psi_{a\mathbf{k}} \rangle$  with  $H_{\mathbf{k}}^{\text{BdG}} \equiv H_{\mathbf{k},\mathbf{0}}^{\text{BdG}}$  and the Fermi-distribution function  $f(E)$ . The derivation of Eq. (4) is shown in Appendix A. When the anapole moment in superconductors  $T_\mu$  is finite, a superconducting state due to Cooper pairs with finite center of mass momenta becomes most stable.

To obtain further insights, using the Bloch wave function which follows  $H_{\mathbf{k}} | u_{n\chi\mathbf{k}} \rangle = \epsilon_{n\mathbf{k}} | u_{n\chi\mathbf{k}} \rangle$ , we expand  $| \psi_a(\mathbf{k}) \rangle$  as  $| \psi_{a\mathbf{k}} \rangle = (\sum_{n,\chi} \phi_{n\chi\mathbf{k}}^{a+} | u_{n\chi\mathbf{k}} \rangle \quad \sum_{n,\chi} \phi_{n\chi\mathbf{k}}^{a-} | u_{n\chi\mathbf{k}} \rangle)^T$ . Because of the Kramers degeneracy, we distinguish two degenerate bands by the helicity  $\chi = \uparrow\downarrow$ . Here,  $\phi_{n\chi\mathbf{k}}^{a\pm}$  is the matrix element of the unitary matrix which diagonalizes the band representation of the BdG Hamiltonian. After calculations, the anapole moment Eq. (4) is divided into two parts,

$$T_\mu = T_\mu^{\text{velo}} + T_\mu^{\text{geom}}, \quad (6)$$

where

$$T_\mu^{\text{velo}} = \sum_{\mathbf{k}} \sum_{n,\chi} C_{n\chi n\chi\mathbf{k}} \partial_\mu \epsilon_{n\mathbf{k}}, \quad (7)$$

$$T_\mu^{\text{geom}} = \sum_{\mathbf{k}} \sum_{n \neq m, \chi \chi'} C_{n\chi m\chi'\mathbf{k}} \times (\epsilon_{m\mathbf{k}} - \epsilon_{n\mathbf{k}}) \langle u_{n\chi\mathbf{k}} | \partial_\mu | u_{m\chi'\mathbf{k}} \rangle, \quad (8)$$

$$C_{n\chi m\chi'\mathbf{k}} = \frac{1}{2} \sum_a f(E_{a\mathbf{k}}) (\phi_{n\chi\mathbf{k}}^{a+*} \phi_{m\chi'\mathbf{k}}^{a+} + \phi_{n\chi\mathbf{k}}^{a-*} \phi_{m\chi'\mathbf{k}}^{a-}). \quad (9)$$

$T_\mu^{\text{velo}}$  in Eq. (7) is called the group velocity term as it contains the group velocity  $\partial_\mu \epsilon_{nk}$ . In the next section, using the general two-band model, we show that this term arises from the asymmetric BS. Equation (9) for  $T_\mu^{\text{geom}}$  is named the geometric term because it contains the Berry connection  $\langle u_{n\chi k} | \partial_\mu u_{m\chi' k} \rangle$ . Through the Berry connection in the geometric term, the geometric properties of Bloch electrons may contribute to the anapole moment. Some conditions have to be satisfied for a finite group velocity term, which vanishes in simple models [28]. On the other hand, the geometric term has been overlooked in the previous study. Owing to the geometric term, the anapole superconductivity becomes recognized as a ubiquitous feature of the  $\mathcal{PT}$ -symmetric mixed-parity pairing state in multiband superconductors.

Before going to the next section, we give an intuitive understanding of the origin of anapole superconductivity based on the group velocity and geometric terms. From the viewpoint of symmetry, the anapole moment should arise from an odd structure in the wave-number space. Since the group velocity term comes from  $\mathbf{k}$ -space structure of the band dispersion, i.e.,  $\partial_\mu \epsilon_n(\mathbf{k})$ , this term arises from the odd structure of BS, namely, asymmetric BS. In contrast, the geometric term arises from the  $\mathbf{k}$ -space geometric properties of Bloch wave functions, i.e.,  $\langle u_{n\chi}(\mathbf{k}) | \partial_\mu u_{m\chi'}(\mathbf{k}) \rangle$ . Therefore, the odd structure which does not appear in BS can induce the anapole moment through the geometric term. These intuitive understandings will be justified in the next section. However, readers who are not interested in the detailed discussion about the origin of anapole superconductivity can skip the next section and directly go to Sec. IV, where the anapole superconductivity is demonstrated in the minimal model of  $\text{UTe}_2$ .

### III. ORIGIN OF ANAPOLE SUPERCONDUCTIVITY

#### A. General discussion

Before demonstrating the anapole superconductivity due to quantum geometry, we discuss the physical origin and the microscopic process of the anapole moment using the Ginzburg-Landau (GL) theory. We also discuss their relation to the group velocity and geometric terms. Up to the second order of the gap function  $\Delta_{\mathbf{k}}$ , the anapole moment is given by

$$T_\mu^{\text{GL}} = \frac{1}{\beta} \sum_{k\omega_n} \text{tr} \left[ \mathcal{G}_{k\omega_n}^p \partial_\mu H_k \mathcal{G}_{k\omega_n}^p \Delta_{\mathbf{k}}^g \mathcal{G}_{k\omega_n}^h \Delta_{\mathbf{k}}^{u\dagger} - \mathcal{G}_{k\omega_n}^p \partial_\mu H_k \mathcal{G}_{k\omega_n}^p \Delta_{\mathbf{k}}^{u\dagger} \mathcal{G}_{k\omega_n}^h \Delta_{\mathbf{k}}^g \right] + (g \leftrightarrow u), \quad (10)$$

where  $\text{tr}$  represents the trace over normal-state degrees of freedom. Here,  $\mathcal{G}_{k\omega_n}^{\text{p(h)}}$   $= (i\omega_n \mp H_k)^{-1}$  is the Green function for the particle (hole) part. The derivation of the formula (10) is shown in Appendix B. From this formula, we see that  $\mathcal{P}$ - and  $\mathcal{T}$ -symmetry breaking is needed for the anapole superconductivity (see also Appendix B).

We can rewrite the formula in the Bloch band basis,

$$T_\mu^{\text{GL}} = \frac{1}{\beta} \sum_{k\omega_n} \sum_{nm} \sum_{\chi_n \chi_m \chi_p} C_{nmpk\omega_n}^{\text{GL}} \text{tr} \left[ P_{n\chi_n k} \partial_\mu H_k P_{m\chi_m k} \times \left( \Delta_{\mathbf{k}}^g P_{p\chi_p k} \Delta_{\mathbf{k}}^{u\dagger} - \Delta_{\mathbf{k}}^{u\dagger} P_{p\chi_p k} \Delta_{\mathbf{k}}^g \right) \right] + (g \leftrightarrow u), \quad (11)$$

where  $C_{nmpk\omega_n}^{\text{GL}} = (i\omega_n - \epsilon_{nk})^{-1} (i\omega_n - \epsilon_{mk})^{-1} (i\omega_n + \epsilon_{pk})^{-1}$ , and  $P_{n\chi_n k} = |u_{n\chi_n k}\rangle \langle u_{n\chi_n k}|$  is the projection operator. For  $n = m = p$ , the summand of Eq. (11) vanishes (see Appendix C for details). Therefore, at least two pairs of  $n$ ,  $m$ , and  $p$  must be nonequivalent for a finite contribution to the anapole moment. In other words, two interband processes are necessary for the anapole superconductivity.

The above necessary condition for  $n$ ,  $m$ , and  $p$  can be satisfied in three cases. The first case,  $n = m \neq p$ , corresponds to the group velocity term, and the odd- and even-parity interband pairings play the role of two interband processes. In the following subsection, it is shown that the group velocity term is closely related to the asymmetric BS. The effect of asymmetric BS on the group velocity term is also discussed in Appendix D.

The remaining two cases correspond to the geometric term since the Berry connection is necessary. In the second case,  $n \neq m$  and  $n = p$  (or  $m = p$ ), the Berry connection of Bloch electrons and either odd-parity or even-parity interband pairing play the role of two interband processes. Finally, in the third case,  $n \neq m \neq p \neq n$ , all of the even-parity interband pairing, odd-parity interband pairing, and the Berry connection appear in the contribution to the anapole moment. In both cases, via the Berry connection, the Bloch electrons undergo an interband transition from the initial band to the different band, which is coupled to the initial band through the interband Cooper pairs. Thus, the two or more interband processes, due to the Berry connection and interband Cooper pairs, induce the anapole moment, which is a physical picture of quantum geometry induced anapole superconductivity.

#### B. General two-band model

Next, for a more transparent understanding, we derive the anapole moment in general two-band superconductors with the Kramers degeneracy. Although we here adopt a two-band model, the following results can be applied to any multiband model with multiple bands near the Fermi surface. The normal-state Hamiltonian is written as

$$H_{\mathbf{k}} = h_{0\mathbf{k}} \mathbf{1} + \mathbf{h}_{\mathbf{k}} \cdot \boldsymbol{\gamma}, \quad (12)$$

by using the  $4 \times 4$  gamma matrices  $\boldsymbol{\gamma} = (\gamma_1 \cdots \gamma_5)$  that anticommute with each other. Here,  $h_{0\mathbf{k}}$  and  $\mathbf{h}_{\mathbf{k}} = (h_{1\mathbf{k}} \cdots h_{5\mathbf{k}})$  depend on the details of the model. The energy dispersion is given by  $\epsilon_{\pm, \mathbf{k}} = h_{0\mathbf{k}} \pm |\mathbf{h}_{\mathbf{k}}|$ . Note that the  $4 \times 4$  normal-state Hamiltonian has two bands due to the Kramers degeneracy.

The  $\mathcal{PT}$ -symmetric parity-mixed pair potential is expressed as [28]

$$\Delta_{\mathbf{k}} = \Delta_{\mathbf{k}}^g + \Delta_{\mathbf{k}}^u, \quad (13)$$

$$\Delta_{\mathbf{k}}^g = \eta_{0\mathbf{k}} \mathbf{1} + \boldsymbol{\eta}_{\mathbf{k}} \cdot \boldsymbol{\gamma}, \quad \Delta_{\mathbf{k}}^u = \frac{i}{2} \sum_{ij} \tilde{\eta}_{ijk} \gamma_i \gamma_j, \quad (14)$$

where  $\eta_{0\mathbf{k}}$ ,  $\boldsymbol{\eta}_{\mathbf{k}} = (\eta_{1\mathbf{k}} \cdots \eta_{5\mathbf{k}})$  and  $\tilde{\eta}_{ijk} = -\tilde{\eta}_{jik}$  are the complex valued order parameters for even- and odd-parity pairing channels. Here, taking appropriate  $U(1)$  gauge,  $\eta_{0\mathbf{k}}$  and  $\eta_{i\mathbf{k}}$  are real while  $\tilde{\eta}_{ijk}$  becomes pure imaginary.

Because of the Kramers degeneracy, the particle Green function can be projected to the two degenerate bands as [64]

$$\mathcal{G}_{k\omega_n}^p = a_{k\omega_n} \mathbf{1} + b_{k\omega_n} \tilde{H}_k, \quad (15)$$

$$a_{k\omega_n} = \frac{1}{2} \sum_{\pm} (i\omega_n - h_{0k} \pm |\mathbf{h}_k|)^{-1}, \quad (16)$$

$$b_{k\omega_n} = \frac{1}{2} \sum_{\pm} \mp (i\omega_n - h_{0k} \pm |\mathbf{h}_k|)^{-1}, \quad (17)$$

with  $\tilde{H}_k = (\mathbf{h}_k \cdot \boldsymbol{\gamma})/|\mathbf{h}_k| = \hat{\mathbf{h}}_k \cdot \boldsymbol{\gamma}$ . The hole Green function is also given by

$$\mathcal{G}_{k\omega_n}^h = c_{k\omega_n} \mathbf{1} + d_{k\omega_n} \tilde{H}_k, \quad (18)$$

where  $a_{k\omega_n} = -c_{k-\omega_n}$  and  $b_{k\omega_n} = -d_{k-\omega_n}$ . Hereafter, we omit the  $(\mathbf{k}, \omega_n)$  dependence for simplicity. Inserting these expressions of Green functions into Eq. (10), we get

$$\begin{aligned} T_{\mu}^{\text{GL}} = & \frac{1}{\beta} \sum_{\mathbf{k}} \sum_{\omega_n} (a^2 \text{ctr}[\partial H M_-^{(1)}] + a^2 d \text{tr}[\partial H M_-^{(2)}] \\ & + ab \text{ctr}[\{\partial H, \tilde{H}\} M_-^{(1)}] + ab d \text{tr}[\{\partial H, \tilde{H}\} M_-^{(2)}] \\ & + b^2 \text{ctr}[\tilde{H} \partial H \tilde{H} M_-^{(1)}] + b^2 d \text{tr}[\tilde{H} \partial H \tilde{H} M_-^{(2)}]). \end{aligned} \quad (19)$$

Here, we introduce the  $\mathcal{P}$ - and  $\mathcal{T}$ -odd bilinear products [28,33,64,65],

$$M_-^{(1)} = [\Delta^g, \Delta^{u\dagger}] + (g \leftrightarrow u), \quad (20)$$

$$M_-^{(2)} = [\Delta^g \tilde{H} \Delta^{u\dagger} - \Delta^{u\dagger} \tilde{H} \Delta^g] + (g \leftrightarrow u). \quad (21)$$

According to Eq. (19), the presence of finite bilinear products is a necessary condition for the anapole superconductivity.

One of the bilinear products  $M_-^{(1)}$  is obtained as

$$M_-^{(1)} = \mathbf{m}_1 \cdot \boldsymbol{\gamma}, \quad (22)$$

$$[\mathbf{m}_1]_j = -4 \sum_{i(\neq j)} \text{Im}[\eta_i \tilde{\eta}_{ij}^*]. \quad (23)$$

It has been shown that  $M_-^{(1)}$  is needed for the asymmetric BS [28], and thus,  $\mathbf{m}_1$  represents the role of the asymmetric BS. More specifically, the necessary condition of the asymmetric BS is given by  $\mathbf{m}_1 \cdot \hat{\mathbf{h}} \neq 0$  [28]. To elucidate the origin and physical meaning of another bilinear product  $M_-^{(2)}$ , we introduce the interband and intraband superconducting fitness (SCF) [66,67],  $F_{g(u)}^C$  and  $F_{g(u)}^A$ , which are defined by

$$F_{g(u)}^C = [\tilde{H}, \Delta^{g(u)}], \quad F_{g(u)}^A = \{\tilde{H}, \Delta^{g(u)}\}. \quad (24)$$

Using this, we can rewrite  $M_-^{(2)}$  as

$$\begin{aligned} M_-^{(2)} = & \frac{1}{4} ([F_g^A, \Delta^{u\dagger}] + [F_u^A, \Delta^{g\dagger}] \\ & - \{F_g^C, \Delta^{u\dagger}\} - \{F_u^C, \Delta^{g\dagger}\}) + \text{H.c.} \end{aligned} \quad (25)$$

This means that both interband and intraband pairings lead to a finite bilinear product  $M_-^{(2)}$ . Each term in Eq. (25) is calculated as

$$[F_g^A, \Delta^{u\dagger}] + \text{H.c.} = 2\mathbf{m}_2 \cdot \boldsymbol{\gamma}, \quad (26)$$

$$[F_u^A, \Delta^{g\dagger}] + \text{H.c.} = 2\mathbf{m}_3 \cdot \boldsymbol{\gamma}, \quad (27)$$

$$\{F_g^C, \Delta^{u\dagger}\} + \text{H.c.} = -2\mathbf{m}_3 \cdot \boldsymbol{\gamma} + 2(\mathbf{m}_1 \cdot \hat{\mathbf{h}}) \mathbf{1}, \quad (28)$$

$$\{F_u^C, \Delta^{g\dagger}\} + \text{H.c.} = -2\mathbf{m}_2 \cdot \boldsymbol{\gamma} + 2(\mathbf{m}_1 \cdot \hat{\mathbf{h}}) \mathbf{1}, \quad (29)$$

where

$$[\mathbf{m}_2]_j = -4 \sum_{i(\neq j)} \hat{h}_i \text{Im}[\eta_0 \tilde{\eta}_{ij}^*], \quad (30)$$

$$[\mathbf{m}_3]_j = -2 \sum_{i_1 i_2 i_3 i_4} \varepsilon_{i_1 i_2 i_3 i_4} \hat{h}_{i_1} \text{Im}[\eta_{i_2} \tilde{\eta}_{i_3 i_4}^*]. \quad (31)$$

Here, we use the relationship

$$\gamma_j = \frac{-1}{4!} \sum_{i_1 i_2 i_3 i_4} \varepsilon_{j i_1 i_2 i_3 i_4} \gamma_{i_1} \gamma_{i_2} \gamma_{i_3} \gamma_{i_4}, \quad (32)$$

with the Levi-Civita tensor  $\varepsilon_{i_1 i_2 i_3 i_4 i_5}$ . Inserting these expressions into Eq. (25), we obtain

$$M_-^{(2)} = -(\mathbf{m}_1 \cdot \hat{\mathbf{h}}) \mathbf{1} + (\mathbf{m}_2 + \mathbf{m}_3) \cdot \boldsymbol{\gamma}. \quad (33)$$

The first term comes from the asymmetric BS, which originates from the interband SCF. On the other hand, the second and third terms arise from either the intraband SCF or interband SCF. To be more precise, the term  $\mathbf{m}_2 \cdot \boldsymbol{\gamma}$  ( $\mathbf{m}_3 \cdot \boldsymbol{\gamma}$ ) needs the  $\mathcal{P}$ -even ( $\mathcal{P}$ -odd) intraband SCF or the  $\mathcal{P}$ -odd ( $\mathcal{P}$ -even) interband SCF. This implies that  $\mathbf{m}_2$  ( $\mathbf{m}_3$ ) contains information of even-parity (odd-parity) intraband pairing and odd-parity (even-parity) interband pairing. Thus, introducing the SCF helps understand the role of  $\mathcal{P}$ -even and  $\mathcal{P}$ -odd interband pairings in the anapole superconductivity.

After a tedious but straightforward calculation we can get the group velocity term and geometric term in the GL theory,

$$T^{\text{GL}} = T^{\text{GL:velo}} + T^{\text{GL:geom}}, \quad (34)$$

$$\begin{aligned} T^{\text{GL:velo}} = & \frac{4}{\beta} \sum_{k\omega_n} [(2abc - a^2d - b^2d) \partial h_0 \\ & - (2abd - a^2c - b^2c) \partial |\mathbf{h}|] \mathbf{m}_1 \cdot \hat{\mathbf{h}}, \end{aligned} \quad (35)$$

$$T^{\text{GL:geom}} = \frac{4}{\beta} \sum_{k\omega_n} (a^2 - b^2) |\mathbf{h}| \partial \hat{\mathbf{h}} \cdot [\mathbf{c} \mathbf{m}_1 + d(\mathbf{m}_2 + \mathbf{m}_3)]. \quad (36)$$

It should be noted that the group velocity term contains a factor  $\mathbf{m}_1 \cdot \hat{\mathbf{h}}$ , which is closely related to the asymmetric BS. Therefore, we conclude that the asymmetric BS is an origin of the group velocity term (see also Appendix D for a simple case).

On the other hand, the Berry connection is essential for the geometric term, as Eq. (36) contains  $\partial \hat{\mathbf{h}}$  which makes the Berry connection finite. More specifically, the geometric term arises from various contributions, which are understood by Eq. (36). For the first term of Eq. (36), in addition to the Berry connection, asymmetric BS is also essential in this contribution. In contrast, the second (third) term of Eq. (11) can be finite without even- (odd-)parity interband pairing. Thus, either odd-parity or even-parity interband pairing causes the anapole superconductivity owing to the quantum geometry, although the group velocity term needs both odd-parity and even-parity interband pairing. In other words, whenever the group velocity term is finite, finite Berry connection ensures



the presence of the geometric term. Moreover, even when the group velocity term is absent, the geometric term can be finite due to  $m_2$  and  $m_1$ . Therefore, necessary conditions for the anapole superconductivity are relaxed by appropriately considering the quantum geometric effect, which was neglected in Ref. [28]. Later, we will also show that the anapole moment is dominated by the geometric term at low temperatures.

#### IV. QUANTUM GEOMETRY INDUCED ANAPOLE SUPERCONDUCTIVITY IN $\text{UTe}_2$

In this section, we first show a general theory for anapole superconductivity in locally noncentrosymmetric superconductors (Sec. IV A) and next focus on  $\text{UTe}_2$  (Secs. IV B and IV C).

##### A. Locally noncentrosymmetric superconductors

Many exotic superconductors of recent interest have multiple sublattices which do not lie on the inversion center.  $\text{UTe}_2$  [13] and  $\text{CeRh}_2\text{As}_2$  [68] are examples of such locally noncentrosymmetric superconductors, and a part of materials is listed in a review article [69]. Before demonstrating the quantum geometry induced anapole superconductivity in  $\text{UTe}_2$ , we show that the locally noncentrosymmetric superconductors are generically the platform of anapole superconductivity and clarify the conditions for it. While the following discussions in this subsection are based on the GL expansion, the BCS theory reproduces the results for the anapole moment quantitatively, as shown in Sec. IV C.

We consider the locally noncentrosymmetric two-sublattice model [28], which is adopted as a minimal model for  $\text{UTe}_2$  later,

$$H = \xi \sigma_0 \otimes \tau_0 + w_x \sigma_0 \otimes \tau_x + w_y \sigma_0 \otimes \tau_y + \mathbf{g} \cdot \boldsymbol{\sigma} \otimes \tau_z, \quad (37)$$

$$\Delta^g = \Delta^g \left[ \sum_{\mu=0,x,y} \phi_g^\mu \sigma_0 \otimes \tau_\mu + \mathbf{d}_g^z \cdot \boldsymbol{\sigma} \otimes \tau_z \right], \quad (38)$$

$$\Delta^u = \Delta^u \left[ \sum_{\mu=0,x,y} \mathbf{d}_u^\mu \cdot \boldsymbol{\sigma} \otimes \tau_\mu + \phi_u^z \sigma_0 \otimes \tau_z \right]. \quad (39)$$

Here,  $\sigma_\mu$  and  $\tau_\mu$  are the Pauli matrices for the spin and sublattice spaces,  $\xi$  is the single-particle kinetic energy, and  $\mathbf{g} = (g_x, g_y, g_z)$  is the staggered-type ASOC due to the local  $\mathcal{P}$ -symmetry breaking at atomic sites. For example, in  $\text{UTe}_2$ , U atoms form a ladder structure, which consists of two sublattices lacking the  $\mathcal{P}$  symmetry at the atomic sites. The local point group descends to  $C_{2v}$  from  $D_{2h}$ , and therefore, the Rashba ASOC naturally appears. Since the two sublattices are related by the global  $\mathcal{P}$  symmetry, the Rashba ASOC shows a staggered form proportional to  $\tau_z$ .

The superconducting pair potentials are divided into the spin-singlet component  $\phi_{g(u)}^\mu$  and the spin-triplet component  $\mathbf{d}_{g(u)}^\mu$ . The local inversion symmetry breaking also leads to sublattice-dependent parity mixing of the pair potential. Thus, the sublattice-independent spin-singlet (spin-triplet) pairing component and the staggered spin-triplet (spin-singlet) one

TABLE I. Correspondence between Pauli and Dirac matrices.

Pauli	Dirac
$\sigma \otimes \tau_z$	$(\gamma_1 \ \gamma_2 \ \gamma_3)$
$\sigma \otimes \tau_y$	$(-i\gamma_1\gamma_4 \ -i\gamma_2\gamma_4 \ -i\gamma_3\gamma_4)$
$\sigma \otimes \tau_x$	$(i\gamma_1\gamma_5 \ i\gamma_2\gamma_5 \ i\gamma_3\gamma_5)$
$\sigma \otimes \tau_0$	$(-i\gamma_2\gamma_3 \ i\gamma_1\gamma_3 \ -i\gamma_1\gamma_2)$
$\sigma_0 \otimes \boldsymbol{\tau}$	$(\gamma_4 \ \gamma_5 \ -i\gamma_4\gamma_5)$

coexist in the even-parity (odd-parity) pair potential. To preserve the  $\mathcal{PT}$  symmetry while breaking the  $\mathcal{T}$  symmetry, the relative phase between the complex-valued order parameters  $\Delta^g$  and  $\Delta^u$  is assumed to be  $\pi/2$ , and thus,  $4\text{Im}(\Delta^g \Delta^{u*}) \neq 0$ .

We show the correspondence between the Pauli matrices and the Dirac matrices in Table I [70], from which the condition for anapole superconductivity can be derived based on the discussions in Sec. III. The results are summarized in Table II, where conditions for the finite group velocity term and the geometric term are explicitly presented. Here, we define  $\hat{\mathbf{g}} = \mathbf{g}/|\mathbf{h}|$  and  $\hat{w}_{x(y)} = w_{x(y)}/|\mathbf{h}|$  with  $|\mathbf{h}| =$

 TABLE II. Conditions for the anapole superconductivity in locally noncentrosymmetric systems. The corresponding SCF is also shown. We assume  $4\text{Im}(\Delta^g \Delta^{u*}) \neq 0$ , which is satisfied in the parity-mixed  $\mathcal{T}$ -symmetry breaking superconductors. When an inequality listed in the table is satisfied, (a) the group velocity term and (b) the geometric term are finite.

Condition (Dirac)	Condition (Pauli)	SCF
(a) Group velocity term		
$\partial \epsilon_{\pm} \mathbf{m}_1 \cdot \hat{\mathbf{h}} \neq 0$	$\partial \epsilon_{\pm} \mathbf{d}_g^z \cdot \mathbf{d}_u^{y(x)} \hat{w}_{x(y)} \neq 0$ $\partial \epsilon_{\pm} \phi_g^{y(x)} \phi_u^z \hat{w}_{x(y)} \neq 0$ $\partial \epsilon_{\pm} \phi_g^{y(x)} \mathbf{d}_u^z \cdot \hat{\mathbf{g}} \neq 0$ $\partial \epsilon_{\pm} (\mathbf{d}_g^z \times \mathbf{d}_u^0) \cdot \hat{\mathbf{g}} \neq 0$	$F_g^C, F_u^C \neq 0$
(b) Geometric term		
$\mathbf{m}_1 \cdot \partial \hat{\mathbf{h}} \neq 0$	$\mathbf{d}_g^z \cdot \mathbf{d}_u^{y(x)} \partial \hat{w}_{x(y)} \neq 0$ $\phi_g^{y(x)} \phi_u^z \partial \hat{w}_{x(y)} \neq 0$ $\phi_g^{y(x)} \mathbf{d}_u^{x(y)} \cdot \partial \hat{\mathbf{g}} \neq 0$ $(\mathbf{d}_g^z \times \mathbf{d}_u^0) \cdot \partial \hat{\mathbf{g}} \neq 0$	$F_g^C, F_u^C \neq 0$
$\mathbf{m}_2 \cdot \partial \hat{\mathbf{h}} \neq 0$	$\phi_g^0 \hat{\mathbf{g}} \cdot \mathbf{d}_u^{y(x)} \partial \hat{w}_{x(y)} \neq 0$ $\phi_g^0 \hat{w}_{y(x)} \phi_u^z \partial \hat{w}_{x(y)} \neq 0$ $\phi_g^0 \hat{w}_{y(x)} \mathbf{d}_u^{x(y)} \cdot \partial \hat{\mathbf{g}} \neq 0$ $\phi_g^0 (\hat{\mathbf{g}} \times \mathbf{d}_u^0) \cdot \partial \hat{\mathbf{g}} \neq 0$	$F_g^A, F_u^C \neq 0$
$\mathbf{m}_3 \cdot \partial \hat{\mathbf{h}} \neq 0$	$\hat{\mathbf{g}} \cdot (\mathbf{d}_g^z \times \mathbf{d}_u^{x(y)}) \partial \hat{w}_{y(x)} \neq 0$ $\hat{w}_{x(y)} \mathbf{d}_g^z \cdot \mathbf{d}_u^0 \partial \hat{w}_{y(x)} \neq 0$ $\hat{\mathbf{g}} \cdot (\phi_g^{x(y)} \mathbf{d}_u^0) \partial \hat{w}_{y(x)} \neq 0$ $\hat{w}_{x(y)} (\mathbf{d}_g^z \times \mathbf{d}_u^{x(y)}) \cdot \partial \hat{\mathbf{g}} \neq 0$ $\hat{w}_{x(y)} \phi_g^0 \mathbf{d}_u^0 \cdot \partial \hat{\mathbf{g}} \neq 0$ $(\hat{\mathbf{g}} \times (\phi_g^{x(y)} \mathbf{d}_u^{x(y)})) \cdot \partial \hat{\mathbf{g}} \neq 0$ $(\hat{\mathbf{g}} \times \mathbf{d}_g^z \phi_u^z) \cdot \partial \hat{\mathbf{g}} \neq 0$	$F_g^C, F_u^A \neq 0$

TABLE III. Classification of parity-mixed superconducting states in the  $D_{2h}$  point group symmetry. Direction of anapole moment is shown for the anapole superconducting state. The other pairing states are monopole superconducting states and represented as ‘‘monopole.’’

	$A_g$	$B_{1g}$	$B_{2g}$	$B_{3g}$
$A_u$	monopole	$T_z$	$T_y$	$T_x$
$B_{1u}$	$T_z$	monopole	$T_x$	$T_y$
$B_{2u}$	$T_y$	$T_x$	monopole	$T_z$
$B_{3u}$	$T_x$	$T_y$	$T_z$	monopole

$\sqrt{w_x^2 + w_y^2 + |\mathbf{g}|^2}$ . Note that all the terms of anapole moment are proportional to  $4\text{Im}(\Delta^g \Delta^{u*})$ , which is finite by assumption. The geometric term can be finite in a relatively simple situation. For example, the  $\mathbf{m}_2$  term gives a finite anapole moment when  $\phi_g^0(\hat{\mathbf{g}} \times \mathbf{d}_u^0) \cdot \partial \hat{\mathbf{g}} \neq 0$ . This condition is satisfied in the presence of an usual spin-singlet pairing component  $\phi_g^0$  and an interband pairing component  $\hat{\mathbf{g}} \times \mathbf{d}_u^0$  when the corresponding Berry connection is finite. If the  $s + ip$ -wave pairing state is realized in  $\text{UTe}_2$  as proposed [14], the even-parity  $s$ -wave component,  $\phi_g^0$ , and the odd-parity  $p$ -wave component,  $\mathbf{d}_u^0$ , naturally exist, and the Berry connection arises from the staggered Rashba ASOC. Thus, the anapole superconductivity is likely to occur in  $\text{UTe}_2$  owing to the quantum geometry when the  $s + ip$ -wave state is stabilized.

### B. Symmetry classification in the $D_{2h}$ point group

Here, we show the classification of parity-mixed superconducting states assuming the crystals of  $D_{2h}$  point group symmetry with  $\text{UTe}_2$  in mind. Combination of the four even-parity irreducible representations ( $A_g, B_{1g}, B_{2g}, B_{3g}$ ) and odd-parity ones ( $A_u, B_{1u}, B_{2u}, B_{3u}$ ) gives  $4 \times 4 = 16$  classes of parity-mixed pairing states. They are classified into either the anapole superconductivity or monopole superconductivity.

The anapole superconducting state has the polarity and shares the symmetry with the magnetic toroidal ordered state, while the monopole superconducting state is a superconducting analog of the magnetic monopole state [71]. In the  $D_{2h}$  point group, the order parameter of anapole superconductivity breaks the  $C_2$  rotation symmetry which flips the polar axis. In contrast, the  $C_2$  rotation symmetry of all directions is preserved in the monopole superconducting state, which means that the anapole moment vanishes and the finite- $\mathbf{q}$  pairing states are prohibited.

Table III shows the finite component of the anapole moment for the 12 anapole superconducting states, while we denote ‘‘monopole’’ for the monopole superconducting state. For instance, the  $A_g + iB_{3u}$  pairing state is an anapole superconducting state with the anapole moment along the  $x$  axis. On the other hand, the  $A_g + iA_u$  pairing state is a nonpolar monopole superconducting state, where the anapole moment vanishes.

### C. Anapole superconductivity in $\text{UTe}_2$

In the theoretical calculation which constructs a 24-orbital model for  $\text{UTe}_2$  [14], competing ferromagnetic and antiferromagnetic fluctuations have been shown, implying the competition between the  $s$ -wave and  $p$ -wave pairings. Comparing the theoretical results with the experimentally observed multiple superconducting phases, the parity-mixed  $\mathcal{T}$ -symmetry-broken  $s + ip$ -wave state was proposed for  $\text{UTe}_2$ . Such  $s + ip$ -wave superconducting state was also discussed in experimental studies [72,73]. In this scenario,  $\mathcal{P}$ - and  $\mathcal{T}$ -symmetry breaking necessary for the anapole superconductivity is predicted. To examine the possible anapole superconductivity in  $\text{UTe}_2$ , we adopt a model for  $\text{UTe}_2$  and show unique features which have microscopic origins beyond the GL theory.

Here, one of the purposes is to derive the minimal condition and universal properties of anapole superconductivity, which are independent of the detailed band structure. Therefore, we focus on the sublattice and spin degrees of freedom in  $\text{UTe}_2$ , giving rise to multiple bands near the Fermi level. Actually, most of the following results are independent of the details of band structure, as is also discussed in Sec. V. Thus, we set the normal-state Hamiltonian Eq. (37) as

$$w_x = w_y = 0, \quad (40)$$

$$\xi = t \sum_{\mu} \cos k_{\mu} - \mu, \quad (41)$$

$$\mathbf{g} = \alpha(\sin k_y, -\sin k_x, 0), \quad (42)$$

with  $(t, \mu, \alpha) = (0.2, 0.4, \pm 0.04)$ . In this model, the energy dispersion is given by  $\epsilon_{\pm} = \xi \pm |\mathbf{g}|$ . In Table II, some terms of the anapole moment are first order in  $\mathbf{g}$ , implying that the anapole moment may depend on the sign of the ASOC coupling constant  $\alpha$ . Thus, we examine the two cases,  $\alpha = \pm 0.04$ . We will actually show that the properties of anapole superconductivity depend on the sign of  $\alpha$ .

First, we consider the superconducting pair potential,

$$\Delta^g(T) = \Delta_0(T) \phi_g^0 \sigma_0 \otimes \tau_0, \quad (43)$$

$$\Delta^u(T) = i \Delta_0(T) d_{u,z}^0 \sigma_z \otimes \tau_0, \quad (44)$$

with  $\phi_g^0 = 1$  and  $d_{u,z}^0 = \sin k_y$ , which belongs to the  $A_g + iB_{3u}$  irreducible representation of the  $D_{2h}$  point group. The temperature dependence is assumed to be  $\Delta_0(T) = \Delta_0^{\max} \tanh[1.74\sqrt{(T_c - T)/T}]$ , where  $\Delta_0^{\max} = \frac{3.53}{2} T_c = 0.02$ .

Based on the GL theory, we expect that the group velocity term vanishes in this case, i.e.,  $\mathbf{m}_1 \cdot \hat{\mathbf{h}} = 0$ . However, since the  $\mathbf{d}$  vector for the  $B_{3u}$  representation is not parallel to the  $\mathbf{g}$  vector for the ASOC of the  $C_{2v}$  point group, odd-parity interband pairing is always finite in addition to intraband pairing. In other words,  $\hat{\mathbf{g}} \times \mathbf{d}_u^0 \neq 0$  leads to odd-parity interband pairing. Therefore, the geometric term is finite because the condition  $\mathbf{m}_2 \cdot \partial \hat{\mathbf{h}} = \phi_g^0(\hat{\mathbf{g}} \times \mathbf{d}_u^0) \cdot \partial \hat{\mathbf{g}} \neq 0$  in Table II(b) is satisfied. As a result,  $A_g + iB_{3u}$  representation of superconductivity in  $\text{UTe}_2$  ensures the presence of the quantum geometry induced anapole superconductivity regardless of the size of the interband pairing.

We calculate the anapole moment by Eqs. (6)–(9) and show the temperature dependence of  $T_x$  in Fig. 1(a). Note that

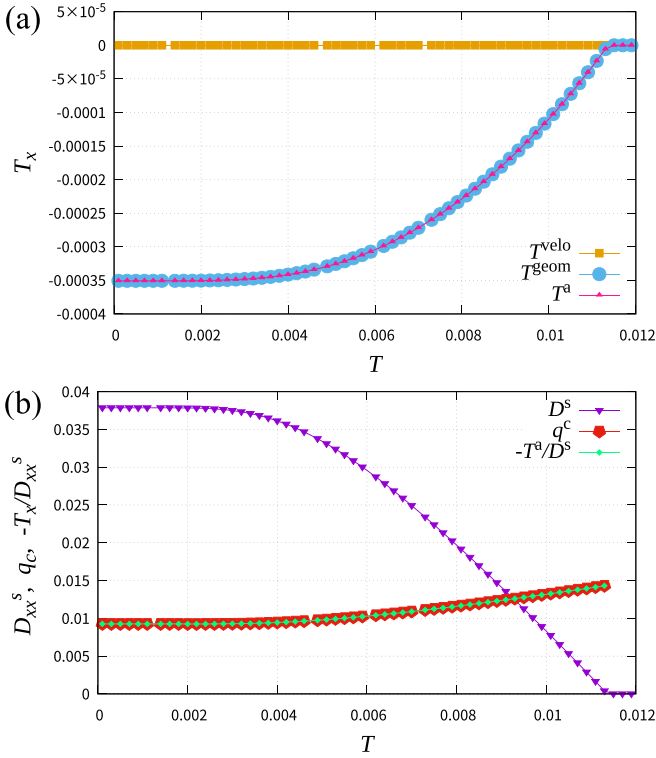


FIG. 1. The temperature dependence of the anapole moment for the pair potential Eqs. (43) and (44). (a) The orange, blue, and pink lines show the group velocity term, geometric term, and total anapole moment, i.e.,  $T_x^{\text{velo}}$ ,  $T_x^{\text{geom}}$ , and  $T_x$ , respectively. The blue and pink lines coincide because  $T_x^{\text{geom}} = T_x$  in this case. (b) The purple and red lines show the superfluid weight  $D_{xx}^s$  and the most stable center of mass momenta of Cooper pairs  $q_c$ . We also show  $-T_x/D_{xx}^s$  by the green line, which almost coincides with the red line for  $q_c$ .

$T_y = T_z = 0$  owing to the symmetry of the  $A_g + iB_{3u}$  irreducible representation (Table III). The anapole moment does not depend on the sign of  $\alpha$  in this case. We denote the total anapole moment as  $T_\mu^a$  in all figures to avoid the confusion with the temperature  $T$ . We find that the group velocity term (orange line) is always zero, revealing that the prediction based on the GL theory is exact. Therefore, the geometric term (blue line) determines the anapole moment (pink line). In Fig. 1(b), we also plot the superfluid weight  $D_{xx}^s$ , defined as the second-order  $\mathbf{q}$  derivative of the free energy at  $\mathbf{q} = 0$  (see Appendix E for details). We can evaluate the center of mass momentum of Cooper pairs in the anapole superconducting state by  $-T_x/D_{xx}^s$  (see Appendix E). We also directly calculate the center of mass momentum  $q_c$ , which minimizes the free energy, and compare it with  $-T_x/D_{xx}^s$  in Fig. 1(b). Since  $-T_x/D_{xx}^s$  almost coincides with  $q_c$ , we confirm that  $-T_x/D_{xx}^s$  provides a good estimation for  $q_c$ , indicating that higher-order  $\mathbf{q}$  derivatives can be ignored. Thus, we conclude that the finite- $\mathbf{q}$  pairing state due to the anapole superconductivity is determined by the anapole moment. We stress that the asymmetric BS does not appear in this model, and the anapole superconductivity has a purely quantum geometric origin. More specifically, the Berry connection of Bloch electrons and the interband pairing play essential roles.

Next, we consider the superconducting pair potential,

$$\Delta^g(T) = \Delta_0(T)(\phi_g^0 \sigma_0 \otimes \tau_0 + d_{g,y}^z \sigma_y \otimes \tau_z), \quad (45)$$

$$\Delta^u(T) = i\Delta_0(T)d_{u,z}^0 \sigma_z \otimes \tau_0, \quad (46)$$

with  $d_{g,y}^z = \sin k_x$ , which also belongs to the  $A_g + iB_{3u}$  irreducible representation. Thus,  $T_y = T_z = 0$  is satisfied as in the previous case. We assume the same temperature dependence of  $\Delta_0(T)$  as before. In this case, the group velocity term becomes finite as expected based on the GL theory since the condition  $\partial(h_0 \pm |\mathbf{h}|)\mathbf{m}_1 \cdot \hat{\mathbf{h}} = \partial\epsilon_{\pm}(d_{g,y}^z \times d_u^0) \cdot \hat{\mathbf{g}} \neq 0$  in Table II(a) is satisfied. Similarly, the geometric term is also finite because  $\mathbf{m}_1 \cdot \partial\hat{\mathbf{h}} = (d_{g,y}^z \times d_u^0) \cdot \partial\hat{\mathbf{g}}$  and  $\mathbf{m}_2 \cdot \partial\hat{\mathbf{h}} = \phi_g^0(\hat{\mathbf{g}} \times d_u^0) \cdot \partial\hat{\mathbf{g}}$  are finite. As the group velocity term is first order in  $\alpha$  according to the GL theory, we expect that the sign of the ASOC coupling constant  $\alpha$  is essential for the group velocity term [74]. In addition, a part of the geometric term due to  $\mathbf{m}_1 \cdot \partial\hat{\mathbf{h}}$  is the first-order term, and the sign of  $\alpha$  also affects the geometric term.

In Figs. 2(a) and 2(b), we show the temperature dependence of the anapole moment for  $\alpha = 0.04$  and  $\alpha = -0.04$ , respectively. We also show the superfluid weight and  $q_c$  in Figs. 2(c) and 2(d). We find that the sign of  $\alpha$  drastically changes the group velocity term, whose sign is opposite between  $\alpha = 0.04$  and  $\alpha = -0.04$ . The magnitude is different between the two cases, provably due to an effect beyond the GL theory. On the other hand, the sign of the Rashba ASOC  $\alpha$  only slightly changes the geometric term. Note that other physical quantities also depend on the sign of  $\alpha$  since the band representation of the gap function depends on  $\alpha$ , as  $\phi_g^0 + d_{g,y}^z \sigma_y / |\mathbf{g}|$ . Actually, we see that the superfluid weight depends on the sign of  $\alpha$ .

In both Figs. 2(a) and 2(b), the group velocity term decays in the low-temperature regime, which is attributed to the fact that the group velocity term is induced by the asymmetric BS. The asymmetric BS, namely,  $E_{ak} \neq E_{a-k}$ , leads to nonequivalent distribution of Bogoliubov quasiparticles,  $f(E_{ak}) \neq f(E_{a-k})$ . This effect mainly induces the group velocity term. However, the Fermi distribution function is reduced to the step function in the low-temperature region,  $f(E_{ak}) \simeq \theta(-E_{ak})$ , which leads to  $f(E_{ak}) \simeq f(E_{a-k})$  in the gapped system and suppresses the group velocity term (see also Appendix D). Therefore, the anapole moment is mainly determined by the geometric term in the low-temperature region. On the other hand, the relation  $\theta(E_{ak}) = \theta(E_{a-k})$  does not hold when the BFS are present. Thus, the group velocity term can be sizable at  $T = 0$  when large BFS appear at  $\mathbf{q} = 0$ . This case is shown in Appendix D.

In the model adopted in this section, while the BFS do not exist at  $\mathbf{q} = 0$ , they appear in the anapole superconducting state as a result of the center of mass momentum of Cooper pairs. In Figs. 3(a) and 3(b), we show the BS in the stable state  $\mathbf{q} = q_c \hat{x}$  for  $\alpha = 0.04$  and  $\alpha = -0.04$ , respectively. In the figures, the inset shows the presence of BFS. In our model for  $\mathbf{q} = 0$ , the spin-triplet pairing component of the pair potential gives rise to the anisotropic gap structure. Therefore, Bogoliubov quasiparticles with almost zero energy are present. As a result, when the anapole moment tilts the BS along the direction of  $\mathbf{q} = q_c \hat{x}$ , the BFS appear near the gap

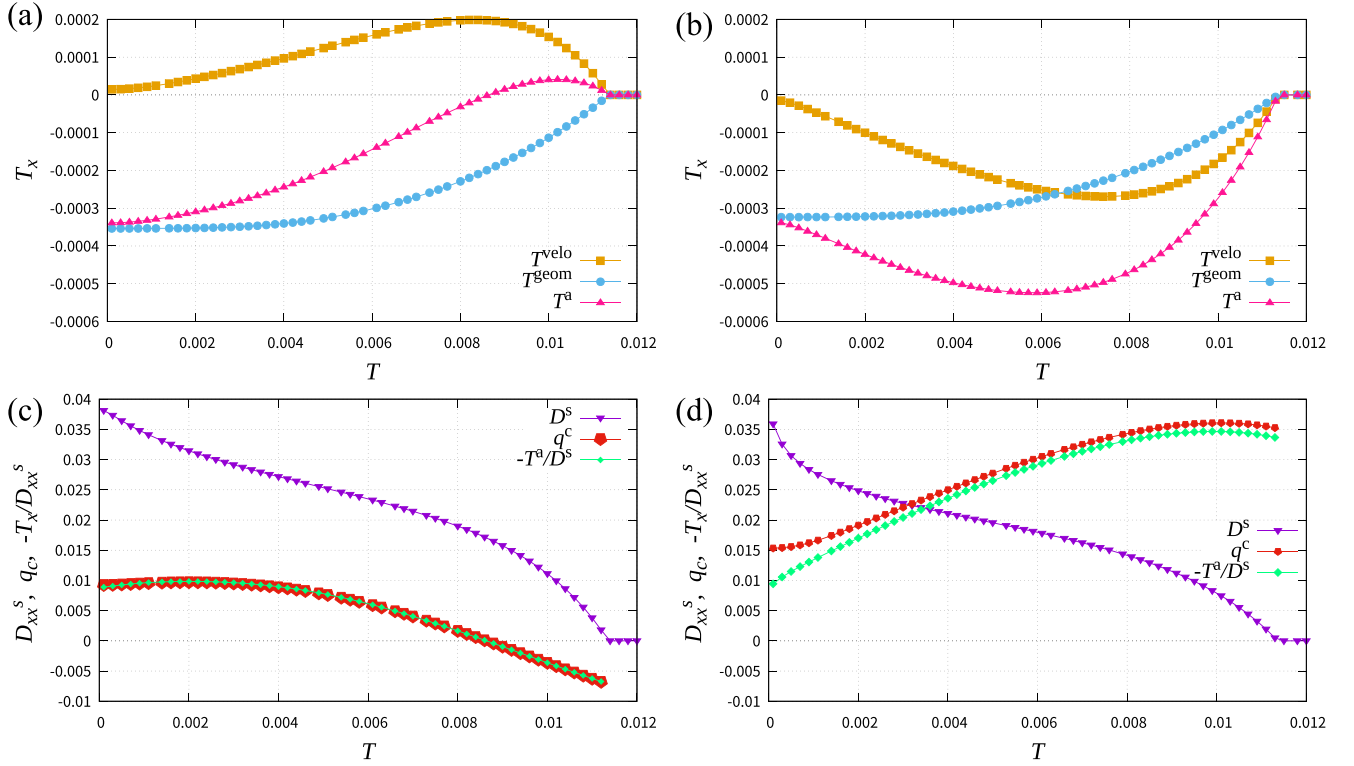


FIG. 2. (a), (b) The anapole moment and (c), (d) the superfluid weight and  $q_c$  for the pair potential Eqs. (45) and (46). We assume  $\alpha = 0.04$  in the panels (a) and (c), while  $\alpha = -0.04$  in (b) and (d). The lines with colors show the same quantities as in Fig. 1.

minimum. Therefore, the anapole superconductivity can be verified by measuring the BFS.

Finally, we show an intriguing phenomenon originating from the competition of the group velocity and geometric terms in the anapole moment. In Figs. 2(a) and 2(c), the anapole moment as well as  $q_c$  change the sign as the temperature decreases. This is because the geometric term has the opposite sign of the group velocity term and the group velocity term vanishes at the zero temperature. As we mentioned above, the BFS are absent when the anapole moment is small  $T_x \simeq 0$ , while they appear for large  $T_x$ . Therefore, the

BFS appear below  $T = T_c$ , disappear in the intermediate temperature region, and reappear in the low-temperature region by following the nonmonotonic temperature dependence of the anapole moment. This is confirmed by the temperature dependence of the DOS in Fig. 4. The DOS at the Fermi level is zero around  $T = 0.0085$  since the anapole moment is small. On the other hand, the DOS is finite in the high- and low-temperature regions where the magnitude of the anapole moment is sizable. This behavior is consistent with the reappearance of BFS, which is a characteristic feature of the anapole superconducting state with competing group velocity

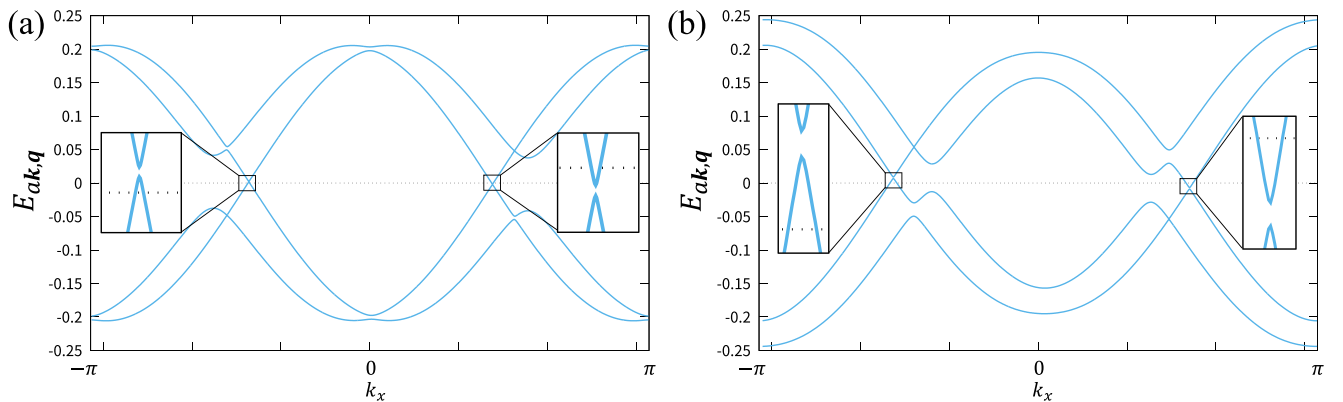


FIG. 3. BS in the anapole superconducting state with  $\mathbf{q} = q_c \hat{x}$  for the pair potential Eqs. (45) and (46). Here, we plot  $E_{ak,q}$  which follows the eigenvalue equation  $H_{k,q}^{\text{BdG}} |\psi_{ak,q}\rangle = E_{ak,q} |\psi_{ak,q}\rangle$ . (a) BS on the line  $(k_y, k_z) = (-0.0713998, 0)$  for  $\alpha = 0.04$  and  $T = 0.002$ . (b) BS on the line  $(k_y, k_z) = (0.499799, 0)$  for  $\alpha = -0.04$  and  $T = 0.01$ . The inset shows the enlarged view, which underlines the presence of BFS.



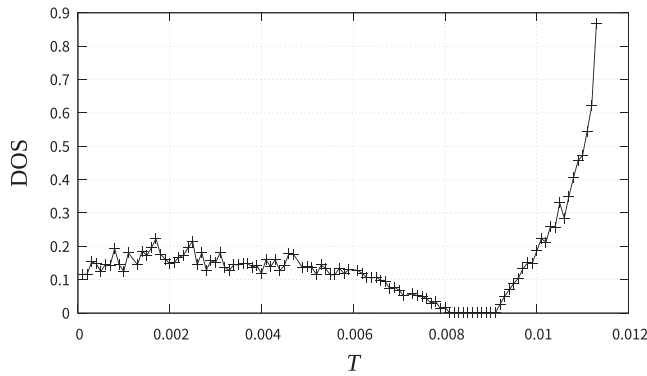


FIG. 4. The temperature dependence of the DOS at the Fermi level calculated by  $\sum_k \sum_a \delta/\pi(\delta^2 + E_{ak,q_c}^2)$  with  $\delta = 1 \times 10^{-6}$ . We assume the same parameters as Figs. 2(a) and 2(c).

and geometric terms. Thus, the role of quantum geometry on anapole superconductivity can be studied by measuring the zero-energy DOS.

## V. DISCUSSION

In this paper, we showed some unique features of quantum geometry induced anapole superconductivity. A candidate material is  $UTe_2$  and our result may pave the way for clarifying the symmetry of superconductivity in  $UTe_2$ . Thus, toward the experimental verification of anapole superconductivity in  $UTe_2$ , we give some discussions in this section.

A concern which is not limited to  $UTe_2$  is the stability of finite- $q$  pairing against the quantum fluctuation. For the  $s$ -wave superconductivity in the isotropic and continuum model, the mean-field solution of the FFLO superconductivity is known to be unstable due to the quantum fluctuation [75,76]. This is attributed to the infinite degeneracy of finite- $q$  pairing states ensured by the isotropic symmetry. In contrast, in the anapole superconductivity, the stable momentum of Cooper pairs  $q$  is restricted to only one direction, and additional degeneracy does not occur. Therefore, it is expected that anapole superconductivity is stable against quantum fluctuation. The argument is also supported by the fact that the finite- $q$  pairing state is stable in the anisotropic three-dimensional system [76]. Our main target is the anisotropic three-dimensional systems, the case of  $UTe_2$ .

Then, we give some comments and remarks on the results relating to  $UTe_2$ , which include (1) the justification of the results obtained by the simplified model, (2) future issues, (3) methods for observing the anapole superconductivity, and (4) the relationship between our results and the recent experiments.

(1) In this paper, we dealt with a simplified model for  $UTe_2$ , where the orbital degree of freedom, electron correlation effect, detailed band structure, and so on are neglected for simplicity. Therefore, we discuss the situations in which our results are adaptable. First, to derive the quantum geometry induced anapole superconductivity in  $UTe_2$ , we only assumed the presence of the ASOC due to the locally noncentrosymmetric structure as the characteristic normal-state property. Since the presence of the ASOC is universal for the crystal

structure of  $UTe_2$ , we conclude that quantum geometry induced anapole superconductivity is also realized in more complicated models for  $UTe_2$ . Also, the decay of the group velocity term is universal when the BFS is absent for the zero center of mass momenta of Cooper pairs. Therefore, these results are adaptable for a wide range of the models for  $UTe_2$ .

Next, we comment on the BFS induced by the anapole moment and the sign change of the center of mass momenta, which are model-dependent. For the BFS to appear from the anapole moment, there must be gap minimum or node which depends on the Fermi surface and the order parameters. Such gap minimum or node is realistic and often obtained in microscopic calculations. Especially, we would like to note that highly anisotropic momentum dependence in both even-parity and odd-parity pair potentials have been obtained based on the periodic Anderson model for  $UTe_2$  [14]. As for the sign change, competition between the geometric and group velocity terms is needed, which also depends on the band structure and order parameters. In addition, in our model the presence or absence of the sign change depends also on the ASOC, which is hard to be predicted. As a result, the sign change of the center of mass momenta and the associated reentrant BFS depend on the model. Thus, the BFS is likely to appear if the anapole superconductivity is realized in  $UTe_2$ , but the reappearing behavior of the BFS is not universal and should be verified by further calculations.

(2) From the above discussion, it is desired to study a more realistic model for  $UTe_2$ , as we have carried out for FeSe based on the first-principles calculation [59,63]. In a model taking account of various degrees of freedom, we may obtain significant contributions from the quantum geometry. Our previous study [63] has shown that the band degeneracy near the Fermi surfaces induces a large geometric contribution to the superfluid weight, implying that the band degeneracy may also be advantageous for the quantum geometry induced anapole superconductivity.

It is also desired to solve multiple gap equations self-consistently, determining the amplitude and temperature dependence of two-component gap functions. While the necessary condition of the anapole superconductivity does not depend on such details, the self-consistent calculation of realistic models may enable quantitative estimation of the anapole moment, which, in turn, predicts the presence/absence of the sign change of the anapole moment. Such quantitative studies are beyond the scope of this paper and are left for future works.

(3) The anapole superconductivity can also be verified by other methods. For example, the Josephson junction experiment, which was proposed to detect the helical superconductivity [45,46], can apply to observe the anapole superconductivity. In addition, some of the authors proposed a unique vortex structure on anapole domains, current-induced anapole domain switching [28], and nonreciprocal optical and Meissner responses [77,78]. Recently, we also showed the superconducting piezoelectric effect [43] and intrinsic superconducting diode effect [79] in the anapole superconductors, which will be presented in another publication [44].

(4) We would like to stress that the symmetry of superconductivity in  $UTe_2$  is unsettled. One of the unresolved issues is the  $T$ -symmetry breaking in the superconducting state,

reported by the STM [80] and the polar Kerr effect [81]. Here we comment on the unidirectional property observed in the STM. It may be related to the anapole superconductivity, which is a unidirectional superconducting state in the bulk. Further studies are desired and ongoing to elucidate the exotic superconductivity in  $\text{UTe}_2$ .

While we focused on the superconducting state at the zero magnetic field in this paper, an anapole superconducting state with finite- $q$  pairing may also appear at finite magnetic fields. The observation of the double superconducting transitions in  $\text{UTe}_2$  under the magnetic field along the  $b$  axis implies the superconducting phases with distinct symmetry [72,73]. If the superconducting state around  $H_b \simeq 15$  T is the  $s + ip$ -wave pairing state as discussed [72], it is either finite- $q$  anapole superconductivity or monopole superconductivity. Although the  $\mathcal{PT}$  symmetry is broken by the magnetic field in this phase, it does not suppress the finite- $q$  pairing. The possibility of anapole superconductivity under the magnetic field is also discussed in Ref. [73].

## VI. SUMMARY

In this paper, we showed that the quantum geometry of Bloch electrons induces the anapole superconductivity when the superconducting state breaks the  $\mathcal{P}$  and  $\mathcal{T}$  symmetry and has the polar symmetry. Formulating the anapole moment characterizing the anapole superconductivity thoroughly, we find the group velocity term and geometric term with different origins. Based on the theory a model for  $\text{UTe}_2$  was analyzed, and characteristic features of anapole superconductivity were clarified.

We identified microscopic processes for the group velocity term and geometric term of the anapole moment. At least two interband processes are necessary. The previous study [28] revealed that the asymmetric BS can induce the anapole superconductivity. This mechanism corresponds to the group velocity term. For the interband processes both even-parity and odd-parity pair potentials must have interband components. In contrast, the normal-state Berry connection represents the interband process and gives rise to the geometric term. Since quantum geometry arises from the geometric structure of Bloch wave functions, the geometric term does not need the asymmetric structure of BS. Even when the odd structure of Cooper pairs does not affect the BS, the geometric term can be finite and cause the anapole superconductivity. In other words, the quantum geometry can extract the odd structure of Cooper pairs which does not appear in the BS, and reflect it in the anapole moment. Therefore, the anapole superconductivity may have a quantum geometric origin. This case requires only either even-parity or odd-parity interband pair potential.

Furthermore, we clarified the general and unique features of anapole superconductivity. First, in the low-temperature region, the anapole superconductivity is purely induced by the quantum geometry. This is because the group velocity term is suppressed by the superconducting gap. In other words, the quantum geometry is needed for the anapole superconductivity in the ground state. Second, the BFS appears in the anapole superconducting state, when the gap is sufficiently anisotropic. Third, when the group velocity term and the

geometric term are competing, the anapole moment changes the sign as decreasing the temperature. This sign change may lead to the nonmonotonic evolution of the BFS. A candidate superconductor  $\text{UTe}_2$  may host an anisotropic superconducting gap [13], and therefore, the appearance of the BFS is expected. Observation of the BFS and their unique temperature dependence would not only evidence the anapole superconductivity in  $\text{UTe}_2$  but also provide a strong constraint on the symmetry of superconductivity (see Table III for symmetry classification of parity-mixed superconducting states). Therefore, search for BFS in  $\text{UTe}_2$  is desirable.

In conclusion, the quantum geometry ubiquitously induces the anapole superconductivity in the  $\mathcal{PT}$ -symmetric parity-mixed pairing state in multiband superconductors. The anapole superconducting state may show unique phenomena which can be experimentally tested. Thus, we propose a way to clarify the superconducting state in  $\text{UTe}_2$ .

## ACKNOWLEDGMENTS

We are grateful to A. Daido, R. Sano, D. Aoki, J.-P. Brison, K. Ishida, Y. Tokiwa, Y. Tokunaga, and D. F. Agterberg for fruitful discussions. This work was supported by JSPS KAKENHI (Grants No. JP18H01178, No. JP18H05227, No. JP20H05159, No. JP21K18145, No. JP22H01181, No. JP22J22520, and No. JP22H04933), JST SPRING (Grant No. JPMJSP2110), and SPIRITS 2020 of Kyoto University.

## APPENDIX A: DERIVATION OF ANAPOLE MOMENT

In this section, we derive the anapole moment in the superconducting state. We start from the BdG Hamiltonian written as

$$\hat{H}^{\text{BdG}} = \frac{1}{2} \sum_k \hat{\Psi}_{k,q}^\dagger \tilde{H}_{k,q}^{\text{BdG}} \hat{\Psi}_{k,q}, \quad (\text{A1})$$

$$\tilde{H}_{k,q}^{\text{BdG}} = \begin{pmatrix} H_{k+q} & \Delta_k U_{\mathcal{T}} \\ U_{\mathcal{T}}^\dagger \Delta_k^\dagger & -H_{-k+q}^T \end{pmatrix}, \quad (\text{A2})$$

$$\hat{\Psi}_{k,q}^\dagger = (\hat{c}_{k+q}^\dagger \quad \hat{c}_{-k+q}^T). \quad (\text{A3})$$

Using the unitary operator,

$$U_{\mathcal{T}_{\text{hole}}} = \begin{pmatrix} \sigma_0 \otimes \mathbf{1} & 0 \\ 0 & U_{\mathcal{T}} \end{pmatrix}, \quad (\text{A4})$$

we can rewrite the BdG Hamiltonian as

$$\begin{aligned} \hat{H}^{\text{BdG}} &= \frac{1}{2} \sum_k \hat{\Psi}_{k,q}^\dagger U_{\mathcal{T}_{\text{hole}}}^\dagger U_{\mathcal{T}_{\text{hole}}} \tilde{H}_{k,q}^{\text{BdG}} U_{\mathcal{T}_{\text{hole}}}^\dagger U_{\mathcal{T}_{\text{hole}}} \hat{\Psi}_{k,q} \\ &= \frac{1}{2} \sum_k \hat{\Psi}_{k,q}^\dagger H_{k,q}^{\text{BdG}} \hat{\Psi}_{k,q}. \end{aligned} \quad (\text{A5})$$

Thus, we define the Nambu Green function with Matsubara frequency  $\omega_n$  as  $\mathcal{G}_{k,q,\omega_n}^{\text{BdG}} = [i\omega_n - H_{k,q}^{\text{BdG}}]^{-1}$ . Using this, the free energy is obtained as  $F_q = -\frac{1}{2\beta} \sum_{k\omega_n} \text{Tr} \ln[\mathcal{G}_{k,q,\omega_n}^{\text{BdG}-1}]$ , where  $\text{Tr}$  represents the trace over all internal degrees of freedom. The anapole moment is defined as the first-order coefficient of the superconducting

free energy with respect to  $\mathbf{q}$  [28]:

$$\begin{aligned}
 T_\mu &= \lim_{\mathbf{q} \rightarrow 0} \frac{dF_{\mathbf{q}}}{d\mathbf{q}_\mu}, \\
 &= \lim_{\mathbf{q} \rightarrow 0} \left( \partial_{\mathbf{q}_\mu} F_{\mathbf{q}} + \sum_l \partial_{\mathbf{q}_\mu} \Delta_l(\mathbf{q}) \partial_{\Delta_l(\mathbf{q})} F(\mathbf{q}) \right), \\
 &= \lim_{\mathbf{q} \rightarrow 0} \partial_{\mathbf{q}_\mu} F_{\mathbf{q}}, \\
 &= \frac{1}{2\beta} \lim_{\mathbf{q} \rightarrow 0} \sum_{k\omega_n} \text{Tr}[\mathcal{G}_{k,q,\omega_n}^{\text{BdG}} \partial_{\mathbf{q}_\mu} H_{k,q}^{\text{BdG}}], \\
 &= \frac{1}{2\beta} \sum_{k\omega_n} \text{Tr}[\mathcal{G}_{k,\omega_n}^{\text{BdG}} \partial_{\mathbf{q}_\mu} H_k^+], \tag{A6}
 \end{aligned}$$

where  $\mathcal{G}_{k,\omega_n}^{\text{BdG}} = \mathcal{G}_{k,q,\omega_n}^{\text{BdG}}|_{\mathbf{q}=0}$ . Here, we use the relationship  $\partial_{\Delta_l(\mathbf{q})} F(\mathbf{q}) = 0$ , in which  $\Delta_l(\mathbf{q})$  denotes the  $\mathbf{k}$ -independent part of each component of the gap function, since the superconducting state is stable. Taking the sum of the Matsubara frequencies, we get the formula of the anapole moment as

$$T_\mu = \frac{1}{2} \sum_k \sum_a f(E_{ak}) \langle \psi_{ak} | \partial_{\mathbf{q}_\mu} H_k^+ | \psi_{ak} \rangle. \tag{A7}$$

## APPENDIX B: ANAPOLE MOMENT FROM GL THEORY

Here, we derive the formula of the anapole moment using the GL expansion. Since we focus on the superconducting state, we ignore the free-electron term and rewrite the free energy as

$$\begin{aligned}
 F_{\mathbf{q}} &= -\frac{1}{2\beta} \sum_{k\omega_n} \text{Tr} \ln [\mathcal{G}_{k,q,\omega_n}^{\text{BdG}-1}] \\
 &= -\frac{1}{2\beta} \sum_{k\omega_n} \text{Tr} [\ln(1 - \mathcal{G}_{k,q,\omega_n} \mathcal{V}_k) + \ln(\mathcal{G}_{k,q,\omega_n}^{-1})] \\
 &= \frac{1}{2\beta} \sum_{c=1}^{\infty} \sum_{k\omega_n} \text{Tr} [\mathcal{G}_{k,q,\omega_n} \mathcal{V}_k \mathcal{G}_{k,q,\omega_n} \mathcal{V}_k]^c + \dots, \tag{B1}
 \end{aligned}$$

where

$$\mathcal{V}_k = \begin{pmatrix} 0 & \Delta_k \\ \Delta_k^\dagger & 0 \end{pmatrix}, \tag{B2}$$

$$\mathcal{G}_{k,q,\omega_n}^{-1} = \mathcal{G}_{k,q,\omega_n}^{\text{BdG}-1} + \mathcal{V}_k. \tag{B3}$$

Up to the second order of the superconducting order parameter, the free energy can be written as

$$\begin{aligned}
 F_{\mathbf{q}}^{\text{GL}} &= \frac{1}{2\beta} \sum_{k\omega_n} \text{Tr} [\mathcal{G}_{k,q,\omega_n} \mathcal{V}_k \mathcal{G}_{k,q,\omega_n} \mathcal{V}_k] \\
 &= \frac{1}{2\beta} \sum_{k\omega_n} \text{tr} [\mathcal{G}_{k,q,\omega_n}^{\text{p}} \Delta_k \mathcal{G}_{k,q,\omega_n}^{\text{h}} \Delta_k^\dagger \\
 &\quad + \mathcal{G}_{k,q,\omega_n}^{\text{h}} \Delta_k^\dagger \mathcal{G}_{k,q,\omega_n}^{\text{p}} \Delta_k] \\
 &= \frac{1}{\beta} \sum_{k\omega_n} \text{tr} [\mathcal{G}_{k,q,\omega_n}^{\text{p}} \Delta_k \mathcal{G}_{k,q,\omega_n}^{\text{h}} \Delta_k^\dagger], \tag{B4}
 \end{aligned}$$

with  $\mathcal{G}_{k,q,\omega_n}^{\text{p(h)-1}} = i\omega_n \mp H_{k\pm q}$ . Then, expanding Eq. (B4) with respect to the  $\mathbf{q}$  up to the first order, we get

$$\begin{aligned}
 F_{\mathbf{q}}^{\text{GL}} &= \frac{1}{\beta} \sum_{k\omega_n} \text{tr} [\partial_{\mathbf{q}_\mu} \mathcal{G}_{k,\omega_n}^{\text{p}} \Delta_k \mathcal{G}_{k,\omega_n}^{\text{h}} \Delta_k^\dagger \\
 &\quad - \mathcal{G}_{k,\omega_n}^{\text{p}} \Delta_k \partial_{\mathbf{q}_\mu} \mathcal{G}_{k,\omega_n}^{\text{h}} \Delta_k^\dagger] q_\mu + \dots \\
 &= \frac{1}{\beta} \sum_{k\omega_n} \text{tr} [\mathcal{G}_{k,\omega_n}^{\text{p}} \partial_{\mathbf{q}_\mu} H_k \mathcal{G}_{k,\omega_n}^{\text{p}} \Delta_k \mathcal{G}_{k,\omega_n}^{\text{h}} \Delta_k^\dagger \\
 &\quad + \mathcal{G}_{k,\omega_n}^{\text{p}} \Delta_k \mathcal{G}_{k,\omega_n}^{\text{h}} \partial_{\mathbf{q}_\mu} H_k \mathcal{G}_{k,\omega_n}^{\text{h}} \Delta_k^\dagger] q_\mu + \dots. \tag{B5}
 \end{aligned}$$

Here, we use  $\partial_{\mathbf{q}_\mu} \mathcal{G}_{k,\omega_n}^{\text{p(h)}} = (-) \mathcal{G}_{k,\omega_n}^{\text{p(h)}} \partial_{\mathbf{q}_\mu} H_k \mathcal{G}_{k,\omega_n}^{\text{p(h)}}$ . Using the relationship,  $\mathcal{G}_{k\omega_n}^{\text{p}} = -\mathcal{G}_{k-\omega_n}^{\text{h}}$ , we obtain

$$\begin{aligned}
 T_\mu^{\text{GL}} &= \frac{1}{\beta} \sum_{k\omega_n} \text{tr} [\mathcal{G}_{k\omega_n}^{\text{p}} \partial_{\mathbf{q}_\mu} H_k \mathcal{G}_{k\omega_n}^{\text{p}} \Delta_k \mathcal{G}_{k\omega_n}^{\text{h}} \Delta_k^\dagger \\
 &\quad - \mathcal{G}_{k\omega_n}^{\text{p}} \partial_{\mathbf{q}_\mu} H_k \mathcal{G}_{k\omega_n}^{\text{p}} \Delta_k^\dagger \mathcal{G}_{k\omega_n}^{\text{h}} \Delta_k]. \tag{B6}
 \end{aligned}$$

In the remaining part of this section, we discuss the symmetry constraint on the anapole moment and simplify Eq. (B6). We assume that the normal-state Hamiltonian is  $\mathcal{P}$  and  $\mathcal{T}$  symmetric, i.e.,  $H_k \xrightarrow{\mathcal{P}} U_{\mathcal{P}} H_{-k} U_{\mathcal{P}}^\dagger = H_k$  and  $H_k \xrightarrow{\mathcal{T}} U_{\mathcal{T}} H_{-k}^* U_{\mathcal{T}}^\dagger = H_k$ , where  $U_{\mathcal{P}}$  is the unitary operator for the  $\mathcal{P}$  symmetry. Here, we require that the  $\mathcal{T}$  operator commute with the  $\mathcal{P}$  operator, i.e.,  $U_{\mathcal{T}} \mathcal{K} U_{\mathcal{P}} = U_{\mathcal{T}} U_{\mathcal{P}}^* \mathcal{K} = U_{\mathcal{P}} U_{\mathcal{T}} \mathcal{K}$  with complex conjugate operator  $\mathcal{K}$  and the  $\mathcal{P}$  operator is its own inverse, i.e.,  $U_{\mathcal{P}}^2 = \mathbf{1}$ . In addition, the  $\mathcal{T}$  operator satisfies  $U_{\mathcal{T}} \mathcal{K} U_{\mathcal{T}} \mathcal{K} = U_{\mathcal{T}} U_{\mathcal{T}}^* = -\mathbf{1}$ , since we consider spinful electron systems.

Let us consider the  $\mathcal{T}$  symmetry in the superconducting state. Under the  $\mathcal{T}$  operation, the pair potential follows  $\Delta_k U_{\mathcal{T}} \xrightarrow{\mathcal{T}} U_{\mathcal{T}} \Delta_{-k}^* U_{\mathcal{T}}^* U_{\mathcal{T}}^T$ . The fermionic antisymmetry,  $\Delta_k U_{\mathcal{T}} = -U_{\mathcal{T}}^T \Delta_{-k}^T$ , leads to  $U_{\mathcal{T}} \Delta_{-k}^* U_{\mathcal{T}}^* U_{\mathcal{T}}^T = -\Delta_k^\dagger U_{\mathcal{T}}^T = \Delta_k^\dagger U_{\mathcal{T}}$  since  $U_{\mathcal{T}} U_{\mathcal{T}}^* = -\mathbf{1}$  is satisfied, which means  $\Delta_k \xrightarrow{\mathcal{T}} \Delta_k^\dagger$ . As a result, when the pair potential is  $\mathcal{T}$  symmetric, the first term of Eq. (B6) cancels out the second term, and therefore, the anapole moment vanishes.

Next, we consider the  $\mathcal{P}$  symmetry. Since  $U_{\mathcal{T}} U_{\mathcal{P}}^* = U_{\mathcal{P}} U_{\mathcal{T}}$  and  $U_{\mathcal{P}}^2 = \mathbf{1}$  lead to  $U_{\mathcal{P}} U_{\mathcal{T}} = U_{\mathcal{T}} U_{\mathcal{P}}^T$ , the pair potential follows  $\Delta_k U_{\mathcal{T}} \xrightarrow{\mathcal{P}} U_{\mathcal{P}} \Delta_{-k} U_{\mathcal{T}} U_{\mathcal{P}}^T = U_{\mathcal{P}} \Delta_{-k} U_{\mathcal{P}}^\dagger U_{\mathcal{T}}$ , which means  $\Delta_k \xrightarrow{\mathcal{P}} U_{\mathcal{P}}^\dagger \Delta_{-k} U_{\mathcal{P}} = \Delta_{gk} - \Delta_{uk}$ . Therefore, because of  $U_{\mathcal{P}} \mathcal{G}_{k\omega_n}^{\text{p(h)}} U_{\mathcal{P}}^\dagger = \mathcal{G}_{k\omega_n}^{\text{p(h)}}$  and  $U_{\mathcal{P}} \partial_{-\mu} H_{-k} U_{\mathcal{P}}^\dagger = -\partial_{\mu} H_k$  with  $\partial_{-\mu} = \frac{\partial}{\partial(-k_\mu)}$ , the  $\mathcal{P}$ -even part of the effective anapole moment,

$$\begin{aligned}
 T_\mu^{\text{GL:even}} &= \frac{1}{\beta} \sum_{k\omega_n} \text{tr} [\mathcal{G}_{k\omega_n}^{\text{p}} \partial_{\mathbf{q}_\mu} H_k \mathcal{G}_{k\omega_n}^{\text{p}} \Delta_k^g \mathcal{G}_{k\omega_n}^{\text{h}} \Delta_k^{g\dagger} \\
 &\quad - \mathcal{G}_{k\omega_n}^{\text{p}} \partial_{\mathbf{q}_\mu} H_k \mathcal{G}_{k\omega_n}^{\text{p}} \Delta_k^{u\dagger} \mathcal{G}_{k\omega_n}^{\text{h}} \Delta_k^u] + (g \leftrightarrow u), \tag{B7}
 \end{aligned}$$

vanishes due to the cancellation between  $\mathbf{k}$  and  $-\mathbf{k}$ . Thus, only the  $\mathcal{P}$ -odd and  $\mathcal{T}$ -odd part of the anapole moment becomes finite and we arrive at Eq. (10) in the main text.

### APPENDIX C: INTERBAND EFFECT ON ANAPOLE MOMENT

Here, we show that at least two interband processes are needed for the anapole moment. We start from Eq. (11) based on the GL theory and consider the contribution from the purely intraband process, namely, the case  $n = m = p$ . Below, the  $\mathbf{k}$  dependence is omitted for simplicity. When  $\chi_n = \chi_m = \chi_p$  is satisfied, the first and second terms of Eq. (11) obviously cancel out each other. Therefore, we consider the other cases.

First, when we fix the U(1) gauge of the Bloch wave function, we can define the relationship between the Kramers doublet through the  $\mathcal{PT}$  symmetry as  $U_{\mathcal{PT}}|u_{n\uparrow}^*\rangle = |u_{n\downarrow}\rangle$  with  $U_{\mathcal{PT}} = U_{\mathcal{P}}U_{\mathcal{T}}$ ; this leads to  $-|u_{n\uparrow}\rangle = U_{\mathcal{PT}}|u_{n\downarrow}^*\rangle$  because of  $U_{\mathcal{PT}}U_{\mathcal{PT}}^* = -1$ . As a result, in the case of  $\chi_n \neq \chi_m$ , the velocity operator of the normal state vanishes as follows:

$$\begin{aligned} \langle u_{n\chi_n} | \partial H | u_{n\chi_m} \rangle &= (\langle u_{n\chi_m} | \partial H | u_{n\chi_n} \rangle)^* \\ &= \langle u_{n\chi_m}^* | \partial H^* | u_{n\chi_n}^* \rangle \\ &= \langle u_{n\chi_m}^* | U_{\mathcal{PT}}^\dagger U_{\mathcal{PT}} \partial H^* U_{\mathcal{PT}}^\dagger U_{\mathcal{PT}} | u_{n\chi_n}^* \rangle \\ &= -\langle u_{n\chi_n} | \partial H | u_{n\chi_m} \rangle \\ &= 0, \end{aligned} \quad (\text{C1})$$

since either  $\chi_n$  or  $\chi_m$  corresponds to the state  $\downarrow$ . Therefore, the contribution to Eq. (11) vanishes, and we have only to consider the rest case,  $\chi_n = \chi_m \neq \chi_p$ . In this case, contribution to Eq. (11) from each  $\mathbf{k}$  and  $\omega_n$  can be written as

$$\begin{aligned} \frac{1}{\beta} \sum_{n, \chi_n \neq \chi_p} C_{nmn}^{\text{GL}} \partial \epsilon_n (\langle u_{n\chi_n} | \Delta^g | u_{n\chi_p} \rangle \langle u_{n\chi_p} | \Delta^{u\dagger} | u_{n\chi_n} \rangle \\ + \langle u_{n\chi_p} | \Delta_k^{g\dagger} | u_{n\chi_n} \rangle \langle u_{n\chi_n} | \Delta_k^u | u_{n\chi_p} \rangle) - (g \leftrightarrow u). \end{aligned} \quad (\text{C2})$$

Because of  $\Delta^g = \Delta^{g\dagger}$  and  $\Delta^u = -\Delta^{u\dagger}$  except for the U(1)-gauge dependence of Cooper pairs, the first and second terms of Eq. (C2) cancel out each other. Thus, we found that the purely intraband process cannot produce the anapole moment. This means that at least two interband effects are needed for the anapole superconductivity, as we discuss in Sec. III A.

### APPENDIX D: GROUP VELOCITY TERM, ASYMMETRIC BS, AND BFS

In this section, we discuss the group velocity term of anapole moment. The following discussions are based on the general two-band model introduced in Sec. III B.

First, we show the close relationship between the group velocity term and asymmetric BS and elucidate the mechanism of the decay of the group velocity term in the low-temperature region. Assuming  $h_{0k} \gg |\mathbf{h}_k|$ , we approximate the velocity operator in the BdG form,

$$\partial_\mu H_k^+ = \partial_\mu h_{0k} \mathbf{1}. \quad (\text{D1})$$

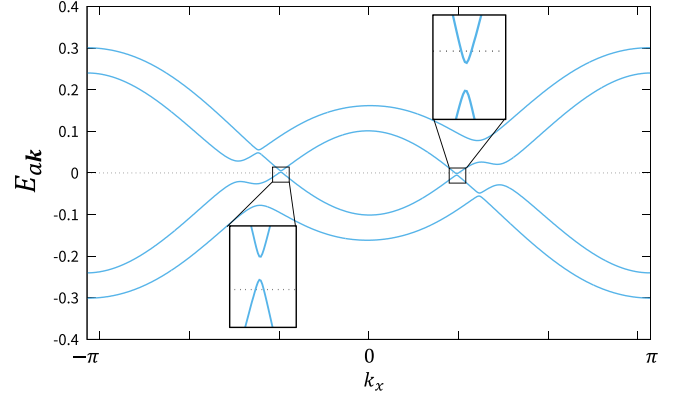


FIG. 5. BS on the line  $(k_y, k_z) = (-0.862398, 0)$ . We assume  $\alpha = 0.04$  and the pair potential in Eqs. (D3) and (D4). Different from Fig. 3 in the main text, we set the center of mass momenta  $\mathbf{q} = 0$ . The inset illustrates the presence of the BFS.

When the polar direction is denoted as  $\mu$ , the anapole moment is obtained from Eq. (4) as

$$\begin{aligned} T_\mu &= \frac{1}{2} \sum_{\mathbf{k}} \sum_a f(E_{a\mathbf{k}}) \partial_\mu h_{0\mathbf{k}} \\ &= \frac{1}{2} \sum_{\mathbf{k} (k_\mu > 0)} \sum_a [f(E_{a\mathbf{k}}) - f(E_{a-\mathbf{k}})] \partial_\mu h_{0\mathbf{k}}, \end{aligned} \quad (\text{D2})$$

which corresponds to the group velocity term since  $\partial_\mu h_{0\mathbf{k}}$  is the group velocity. Thus,  $f(E_{a\mathbf{k}}) - f(E_{a-\mathbf{k}})$ , which represents the asymmetric structure of BS, induces the group velocity term. However, the Fermi distribution function is approximated by the step function,  $f(E_{a\mathbf{k}}) \approx \theta(-E_{a\mathbf{k}})$ , in the low-temperature region, and therefore,  $f(E_{a\mathbf{k}}) - f(E_{a-\mathbf{k}}) = 0$  at the zero temperature when  $E_{a\mathbf{k}}$  and  $E_{a-\mathbf{k}}$  have the same sign. Thus, the group velocity term vanishes at  $T = 0$ , unless the BFS are present.

On the other hand, when the system has the BFS,  $f(E_{a\mathbf{k}}) - f(E_{a-\mathbf{k}}) \neq 0$  even at  $T = 0$ . Thus, we expect that the group velocity term does not completely disappear at  $T = 0$ . To verify this expectation, we consider the superconducting pair potential,

$$\Delta^g(T) = \frac{1}{2} \Delta_0(T) \phi_g^0 \sigma_0 \otimes \tau_0 + \Delta_0(T) d_{g,y}^z \sigma_y \otimes \tau_z, \quad (\text{D3})$$

$$\Delta^u(T) = i \Delta_0(T) d_{u,z}^0 \sigma_z \otimes \tau_0. \quad (\text{D4})$$

The difference from Eqs. (45) and (46) is only the factor 1/2 in the first term of Eq. (D3). We show the BS for  $\mathbf{q} = 0$  in Fig. 5. Different from the cases discussed in Sec. IV C, the BFS appear even for  $\mathbf{q} = 0$ . The temperature dependence of the anapole moment is shown in Fig. 6, and indeed, we see that the group velocity term is not completely suppressed at  $T = 0$ . Thus, the presence of the BFS at  $\mathbf{q} = 0$  enhances the group velocity term, consistent with the above expectation. In this case, the anapole moment at  $T = 0$  is not determined only by the geometric term. Even in this case, the sign change of the anapole moment can occur.



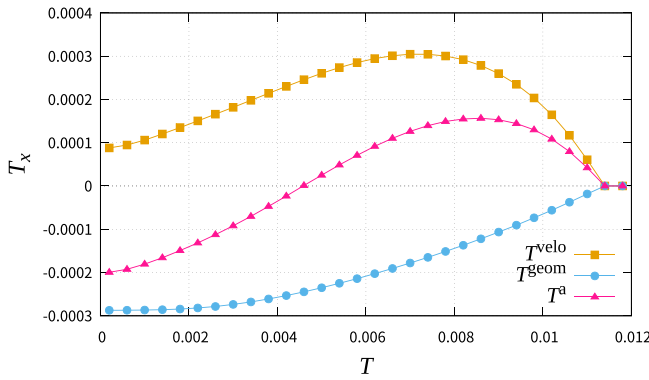


FIG. 6. The temperature dependence of the anapole moment for the pair potential Eqs. (D3) and (D4). All colors show the same quantities as in Fig. 1(a).

### APPENDIX E: SUPERFLUID WEIGHT AND CENTER OF MASS MOMENTA OF COOPER PAIRS

Here, we consider the variation of free energy with respect to the center of mass momentum of Cooper pairs  $q_\mu$  in a direction along which the anapole moment  $T_\mu$  is finite. Up

to the second order of  $q_\mu$ , the superconducting free energy is expressed as

$$F_q = \frac{1}{2} D_{\mu\mu}^s q_\mu^2 + T_\mu q_\mu + F_0. \quad (E1)$$

The superfluid density  $D_{\mu\mu}^s$  is given by the formula [63]

$$D_{\mu\mu}^s = \frac{1}{2} \sum_k \sum_a f(E_{ak}) \langle \psi_{ak} | \partial_\mu \partial_\mu H_k^- | \psi_{ak} \rangle + \frac{1}{2} \sum_k \sum_{ab} \frac{f(E_{ak}) - f(E_{bk})}{E_{ak} - E_{bk}} \times \langle \psi_{ak} | \partial_\mu H_k^+ | \psi_{bk} \rangle \langle \psi_{bk} | \partial_\mu H_k^+ | \psi_{ak} \rangle, \quad (E2)$$

where

$$H_k^- = \begin{pmatrix} H_k & 0 \\ 0 & -H_k \end{pmatrix}. \quad (E3)$$

The superconducting free energy is rewritten as

$$F_q = \frac{1}{2} D_{\mu\mu}^s (q_\mu + T_\mu / D_{\mu\mu}^s)^2 - T_\mu^2 / 2 D_{\mu\mu}^s + F_0. \quad (E4)$$

Thus, the center of mass momentum  $q_c$  realizing the minimum free energy is estimated as  $-T_\mu / D_{\mu\mu}^s$ . This formula is valid when  $q_c$  is small.

- 
- [1] E. Bauer and M. Sigrist (eds.), *Non-Centrosymmetric Superconductors: Introduction and Overview* (Springer, Berlin, 2012).
- [2] M. Smidman, M. B. Salamon, H. Q. Yuan, and D. F. Agterberg, *Rep. Prog. Phys.* **80**, 036501 (2017).
- [3] I. A. Sergienko, *Phys. Rev. B* **69**, 174502 (2004).
- [4] Y. Wang and L. Fu, *Phys. Rev. Lett.* **119**, 187003 (2017).
- [5] W. Yang, C. Xu, and C. Wu, *Phys. Rev. Res.* **2**, 042047(R) (2020).
- [6] P. Goswami and B. Roy, *Phys. Rev. B* **90**, 041301(R) (2014).
- [7] K. Shiozaki and S. Fujimoto, *Phys. Rev. B* **89**, 054506 (2014).
- [8] B. Roy, *Phys. Rev. B* **101**, 220506(R) (2020).
- [9] S. Ryu, J. E. Moore, and A. W. W. Ludwig, *Phys. Rev. B* **85**, 045104 (2012).
- [10] X.-L. Qi, E. Witten, and S.-C. Zhang, *Phys. Rev. B* **87**, 134519 (2013).
- [11] T. Scaffidi, *Phys. Rev. B* **107**, 014505 (2023).
- [12] S. Ran, C. Eckberg, Q.-P. Ding, Y. Furukawa, T. Metz, S. R. Saha, I.-L. Liu, M. Zic, H. Kim, J. Paglione, and N. P. Butch, *Science* **365**, 684 (2019).
- [13] D. Aoki, J.-P. Brison, J. Flouquet, K. Ishida, G. Knebel, Y. Tokunaga, and Y. Yanase, *J. Phys.: Condens. Matter* **34**, 243002 (2022).
- [14] J. Ishizuka and Y. Yanase, *Phys. Rev. B* **103**, 094504 (2021).
- [15] D. Braithwaite, M. Vališka, G. Knebel, G. Lapertot, J.-P. Brison, A. Pourret, M. E. Zhitomirsky, J. Flouquet, F. Honda, and D. Aoki, *Commun. Phys.* **2**, 147 (2019).
- [16] S. Ran, H. Kim, I.-L. Liu, S. R. Saha, I. Hayes, T. Metz, Y. S. Eo, J. Paglione, and N. P. Butch, *Phys. Rev. B* **101**, 140503(R) (2020).
- [17] W.-C. Lin, D. J. Campbell, S. Ran, I.-L. Liu, H. Kim, A. H. Nevidomskyy, D. Graf, N. P. Butch, and J. Paglione, *npj Quantum Mater.* **5**, 68 (2020).
- [18] G. Knebel, M. Kimata, M. Vališka, F. Honda, D. Li, D. Braithwaite, G. Lapertot, W. Knafo, A. Pourret, Y. J. Sato, Y. Shimizu, T. Kihara, J.-P. Brison, J. Flouquet, and D. Aoki, *J. Phys. Soc. Jpn.* **89**, 053707 (2020).
- [19] D. Aoki, F. Honda, G. Knebel, D. Braithwaite, A. Nakamura, D. Li, Y. Homma, Y. Shimizu, Y. J. Sato, J.-P. Brison, and J. Flouquet, *J. Phys. Soc. Jpn.* **89**, 053705 (2020).
- [20] S. M. Thomas, F. B. Santos, M. H. Christensen, T. Asaba, F. Ronning, J. D. Thompson, E. D. Bauer, R. M. Fernandes, G. Fabbris, and P. F. S. Rosa, *Sci. Adv.* **6**, eabc8709 (2020).
- [21] S. M. Thomas, C. Stevens, F. B. Santos, S. S. Fender, E. D. Bauer, F. Ronning, J. D. Thompson, A. Huxley, and P. F. S. Rosa, *Phys. Rev. B* **104**, 224501 (2021).
- [22] C. Duan, K. Sasmal, M. B. Maple, A. Podlesnyak, J.-X. Zhu, Q. Si, and P. Dai, *Phys. Rev. Lett.* **125**, 237003 (2020).
- [23] M. Vališka, W. Knafo, G. Knebel, G. Lapertot, D. Aoki, and D. Braithwaite, *Phys. Rev. B* **104**, 214507 (2021).
- [24] N. P. Butch, S. Ran, S. R. Saha, P. M. Neves, M. P. Zic, J. Paglione, S. Gladchenko, Q. Ye, and J. A. Rodriguez-Rivera, *npj Quantum Mater.* **7**, 39 (2022).
- [25] C. Duan, R. E. Baumbach, A. Podlesnyak, Y. Deng, C. Moir, A. J. Breindel, M. B. Maple, E. M. Nica, Q. Si, and P. Dai, *Nature (London)* **600**, 636 (2021).
- [26] S. Raymond, W. Knafo, G. Knebel, K. Kaneko, J.-P. Brison, J. Flouquet, D. Aoki, and G. Lapertot, *J. Phys. Soc. Jpn.* **90**, 113706 (2021).
- [27] D. V. Ambika, Q.-P. Ding, K. Rana, C. E. Frank, E. L. Green, S. Ran, N. P. Butch, and Y. Furukawa, *Phys. Rev. B* **105**, L220403 (2022).
- [28] S. Kanasugi and Y. Yanase, *Commun. Phys.* **5**, 39 (2022).
- [29] K. I. Wysokiński, J. F. Annett, and B. L. Györfy, *Phys. Rev. Lett.* **108**, 077004 (2012).
- [30] E. Taylor and C. Kallin, *Phys. Rev. Lett.* **108**, 157001 (2012).

- [31] M. Gradhand, K. I. Wysokinski, J. F. Annett, and B. L. Györfy, *Phys. Rev. B* **88**, 094504 (2013).
- [32] D. F. Agterberg, P. M. R. Brydon, and C. Timm, *Phys. Rev. Lett.* **118**, 127001 (2017).
- [33] P. M. R. Brydon, D. F. Agterberg, H. Menke, and C. Timm, *Phys. Rev. B* **98**, 224509 (2018).
- [34] N. A. Spaldin, M. Fiebig, and M. Mostovoy, *J. Phys.: Condens. Matter* **20**, 434203 (2008).
- [35] J. Jeong, Y. Sidis, A. Louat, V. Brouet, and P. Bourges, *Nat. Commun.* **8**, 15119 (2017).
- [36] H. Murayama, K. Ishida, R. Kurihara, T. Ono, Y. Sato, Y. Kasahara, H. Watanabe, Y. Yanase, G. Cao, Y. Mizukami, T. Shibauchi, Y. Matsuda, and S. Kasahara, *Phys. Rev. X* **11**, 011021 (2021).
- [37] H. Watanabe and Y. Yanase, *Phys. Rev. X* **11**, 011001 (2021).
- [38] J. Ahn, G.-Y. Guo, and N. Nagaosa, *Phys. Rev. X* **10**, 041041 (2020).
- [39] V. V. Flambaum, I. B. Khriplovich, and O. P. Sushkov, *Phys. Lett. B* **146**, 367 (1984).
- [40] P. Fulde and R. A. Ferrell, *Phys. Rev.* **135**, A550 (1964).
- [41] A. I. Larkin and Y. N. Ovchinnikov, *Zh. Eksp. Teor. Fiz.* **47**, 1136 (1964). [*Sov. Phys. JETP* **20**, 762 (1965)].
- [42] M. Zegrodnik and P. Wójcik, *Phys. Rev. B* **106**, 184508 (2022).
- [43] M. Chazono, H. Watanabe, and Y. Yanase, *Phys. Rev. B* **105**, 024509 (2022).
- [44] M. Chazono, S. Kanasugi, T. Kitamura, and Y. Yanase, *Phys. Rev. B* **107**, 214512 (2023).
- [45] R. P. Kaur, D. F. Agterberg, and M. Sigrist, *Phys. Rev. Lett.* **94**, 137002 (2005).
- [46] The Josephson effect is proposed for the detection of the phase modulation in the helical superconductivity [45]. We consider that this method is also useful for observing the phase modulation in the anapole superconductivity.
- [47] Y. Matsuda and H. Shimahara, *J. Phys. Soc. Jpn.* **76**, 051005 (2007).
- [48] N. Marzari and D. Vanderbilt, *Phys. Rev. B* **56**, 12847 (1997).
- [49] R. Resta, *Eur. Phys. J. B* **79**, 121 (2011).
- [50] Y. Gao, S. A. Yang, and Q. Niu, *Phys. Rev. Lett.* **112**, 166601 (2014).
- [51] Y. Gao and D. Xiao, *Phys. Rev. Lett.* **122**, 227402 (2019).
- [52] M. F. Lapa and T. L. Hughes, *Phys. Rev. B* **99**, 121111(R) (2019).
- [53] A. Daido, A. Shitade, and Y. Yanase, *Phys. Rev. B* **102**, 235149 (2020).
- [54] A. Julku, G. M. Bruun, and P. Törmä, *Phys. Rev. B* **104**, 144507 (2021).
- [55] A. Julku, G. M. Bruun, and P. Törmä, *Phys. Rev. Lett.* **127**, 170404 (2021).
- [56] D. D. Solnyshkov, C. Leblanc, L. Bessonart, A. Nalitov, J. Ren, Q. Liao, F. Li, and G. Malpuech, *Phys. Rev. B* **103**, 125302 (2021).
- [57] Q. Liao, C. Leblanc, J. Ren, F. Li, Y. Li, D. Solnyshkov, G. Malpuech, J. Yao, and H. Fu, *Phys. Rev. Lett.* **127**, 107402 (2021).
- [58] J.-W. Rhim, K. Kim, and B.-J. Yang, *Nature (London)* **584**, 59 (2020).
- [59] T. Kitamura, J. Ishizuka, A. Daido, and Y. Yanase, *Phys. Rev. B* **103**, 245114 (2021).
- [60] S. Peotta and P. Törmä, *Nat. Commun.* **6**, 8944 (2015).
- [61] L. Liang, T. I. Vanhala, S. Peotta, T. Siro, A. Harju, and P. Törmä, *Phys. Rev. B* **95**, 024515 (2017).
- [62] P. Törmä, S. Peotta, and B. A. Bernevig, *Nat. Rev. Phys.* **4**, 528 (2022).
- [63] T. Kitamura, T. Yamashita, J. Ishizuka, A. Daido, and Y. Yanase, *Phys. Rev. Res.* **4**, 023232 (2022).
- [64] M. D. E. Denys and P. M. R. Brydon, *Phys. Rev. B* **103**, 094503 (2021).
- [65] P. M. R. Brydon, D. S. L. Abergel, D. F. Agterberg, and V. M. Yakovenko, *Phys. Rev. X* **9**, 031025 (2019).
- [66] A. Ramires and M. Sigrist, *Phys. Rev. B* **94**, 104501 (2016).
- [67] A. Ramires, D. F. Agterberg, and M. Sigrist, *Phys. Rev. B* **98**, 024501 (2018).
- [68] S. Khim, J. F. Landaeta, J. Banda, N. Bannor, M. Brando, P. M. R. Brydon, D. Hafner, R. Küchler, R. Cardoso-Gil, U. Stockert, A. P. Mackenzie, D. F. Agterberg, C. Geibel, and E. Hassinger, *Science* **373**, 1012 (2021).
- [69] M. H. Fischer, M. Sigrist, D. F. Agterberg, and Y. Yanase, *Annu. Rev. Condens. Matter Phys.* **14**, 153 (2023).
- [70] The two-orbital model with orbitals of the same (opposite) parity is given by the permutation,  $(\tau_x, \tau_y, \tau_z) \rightarrow (\tau_{z(y)}, \tau_{x(z)}, \tau_{y(x)})$ .
- [71] H. Watanabe and Y. Yanase, *Phys. Rev. B* **98**, 245129 (2018).
- [72] A. Rosuel, C. Marcenat, G. Knebel, T. Klein, A. Pourret, N. Marquardt, Q. Niu, S. Rousseau, A. Demuer, G. Seyfarth, G. Lapertot, D. Aoki, D. Braithwaite, J. Flouquet, and J.-P. Brison, *Phys. Rev. X* **13**, 011022 (2023).
- [73] H. Sakai, Y. Tokiwa, P. Opletal, M. Kimata, S. Awaji, T. Sasaki, D. Aoki, S. Kambe, Y. Tokunaga, and Y. Haga, *Phys. Rev. Lett.* **130**, 196002 (2023).
- [74] Considering that the group velocity term is also the first-order of  $\partial\xi$ , the sign of the  $\partial\xi$ , which is determined by structure of the band dispersion, is also crucial for the group velocity term.
- [75] J. Wang, Y. Che, L. Zhang, and Q. Chen, *Phys. Rev. B* **97**, 134513 (2018).
- [76] P. Zdybel, M. Homenda, A. Chlebicki, and P. Jakubczyk, *Phys. Rev. A* **104**, 063317 (2021).
- [77] H. Watanabe, A. Daido, and Y. Yanase, *Phys. Rev. B* **105**, 024308 (2022).
- [78] H. Watanabe, A. Daido, and Y. Yanase, *Phys. Rev. B* **105**, L100504 (2022).
- [79] A. Daido, Y. Ikeda, and Y. Yanase, *Phys. Rev. Lett.* **128**, 037001 (2022).
- [80] L. Jiao, S. Howard, S. Ran, Z. Wang, J. O. Rodriguez, M. Sigrist, Z. Wang, N. P. Butch, and V. Madhavan, *Nature (London)* **579**, 523 (2020).
- [81] I. M. Hayes, D. S. Wei, T. Metz, J. Zhang, Y. S. Eo, S. Ran, S. R. Saha, J. Collini, N. P. Butch, D. F. Agterberg, A. Kapitulnik, and J. Paglione, *Science* **373**, 797 (2021).